

New insight into the physics of iron pnictides from optical and penetration depth data

S-L Drechsler¹, H Rosner², M Grobosch¹, G Behr¹, F Roth¹,
G Fuchs¹, K Koepernik¹, R Schuster¹, J Malek^{1,3}, S Elgazzar⁴,
M Rotter⁵, D Johrendt⁵, H-H Klauss⁶, B Büchner¹, and
M Knupfer¹

¹ IFW Dresden, P.O. Box 270116, D-01171 Dresden, Germany

² Max-Planck-Institute for Chemical Physics of Solids, Dresden, Germany

³ Institute of Physics, ASCR, Prague, Czech Republic

⁴ Dept. of Physics, Faculty of Science, Menoufia University, Shebin El-kom, Egypt

⁵ University of Munich, Dept. of Chem. & Biochem., D-81377 Munich, Germany

⁶ Institut für Festkörperphysik, TU Dresden, D-01069 Dresden, Germany

E-mail: s.l.drechsler@ifw-dresden.de

Abstract. We report theoretical values for the unscreened plasma frequencies Ω_p of several Fe pnictides obtained from density functional theory (DFT) based calculations within the local density approximation (LDA) and compare them with experimental plasma frequencies obtained from reflectivity measurements on both polycrystalline samples and single crystals. The sizable renormalization observed for all considered compounds points to the presence of significant many-body effects beyond the LDA. From the large values of the empirical background dielectric constant $\varepsilon_\infty \approx 12$ -15 derived from reflectivity data, we estimate a large arsenic polarizability $\tilde{\alpha}_{As} \approx 9.5 \pm 1.2 \text{ \AA}^3$ where the details depend on the polarizabilities of the remaining ions taken from the literature. This large polarizability can significantly reduce the value of the Coulomb repulsion $U_d \sim 4 \text{ eV}$ on iron known from iron oxides to a level of 2 eV or below. In general, independently on such details, this result points to rather strong polaronic effects as suggested by G.A. Sawatzky *et al.*, in references *arXiv:0808.1390* [11] and *arXiv:0811.0214*[12]. Possible consequences for the conditions of a formation of bipolarons are discussed, too. From the extrapolated μ SR (muon spin rotation) penetration depth data at very low-temperature and the experimental value of the unscreened plasma frequency we estimate the total coupling constant λ_{tot} for the electron-boson interaction within the framework of the Eliashberg-theory adopting an effective single band approximation. For $\text{LaFeAsO}_{0.9}\text{F}_{0.1}$ a weak to intermediately strong coupling regime and a quasi-clean limit behaviour are found. For a pronounced multiband case we obtain a constraint for various intraband coupling constants which in principle allows for a sizable strong coupling in bands with either slow electrons or holes.

PACS numbers: 1315, 9440T

Content

1. Introduction	2
2. Reflectivity and its analysis	4
2.1. Studies on polycrystalline samples	4
2.2. BaFe ₂ As ₂ single crystal studies	7
3. FPLO analysis and comparison of unscreened plasma frequencies	10
4. Discussion of possible related microscopic many-body effects	12
4.1. The Mott-Hubbard "bad metal" scenario	12
4.2. The weakly correlated As-polarization scenario	15
5. The <i>el-boson</i> coupling strength and constraints for pairing mechanisms	20
5.1 One-band Eliashberg analysis	20
5.1.1 Comparison with other pnictide superconductors	23
5.1.2 Comparison with other exotic superconductors	25
5.2 Multiband aspects	28
6. Conclusion	29
Acknowledgments	30
References	30

1. Introduction

Naturally, shortly after the discovery [1] of superconductivity at relatively high transition temperatures T_c up to 56 K in several iron pnictide compounds despite all efforts world wide, the underlying pairing mechanism and many basic physical properties both in the superconducting and in the normal state are still debated. This concerns also the nonsuperconducting parent compounds, which often show magnetic phase transitions. In such a situation a combined theoretical and experimental study of selected systems as well as a detailed comparison of various members of the fastly growing family among themselves and also with other more or less exotic superconductors, especially with the high temperature superconducting cuprates (HTSC) might provide useful insight into related problems. In this context the unscreened plasma frequency Ω_p determined from optical measurements or electron energy-loss spectroscopy (EELS) at frequencies near the visible range

$$\Omega_p = \frac{4\pi e^2 n}{m^*} \quad (1)$$

is a physical quantity of central interest in the present paper for several reasons. (i) It provides direct insight in the dynamics of free charge carriers that are responsible for the superconductivity. In particular, it reflects also the possible influence of many-body effects in changing their effective mass m^* and measures the density of paired electrons (condensate or superfluid density), if as in the BCS-case $n = n_s$ holds. (ii) According

to the famous Uemura plot [2] for T_c vs. n_s/m^* , simple linear relations between the two quantities may be expected for many exotic type-II superconductors, and Ω_{pl}^2 would then be a direct measure of T_c . Such plots have been presented both for underdoped HTSC and for the pnictide superconductors as well [2, 3, 4, 5, 6, 7, 8]. In some cases, especially for members of the 122-family, i.e. for Ba(Sr)Fe₂As₂ derived superconductors its applicability has been put in question [8, 9]. Anyhow, since a Bose condensation of bipolarons is naturally directly related to the superfluid density [10], bipolaronic scenarios such as the recently proposed one by G.A. Sawatzky *et al.* [11, 12] are of special interest.

The unscreened plasma frequency is also of considerable interest for the analysis of resistivity ($\rho(T)$) data analyzed within the frequently used Drude model. In particular, the high-temperature linear T -region is often used to extract the transport electron-phonon ($el-ph$) coupling constant λ_{tr} [13] using the simple relation

$$\lambda_{tr} = \frac{\hbar\Omega_p^2}{8\pi^2k_B} \frac{d\rho}{dT}. \quad (2)$$

For standard superconductors λ_{tr} does not differ much from the Fermi surface averaged $el-ph$ coupling constant λ_{el-ph} which governs the transition temperature T_c of the superconducting state and it is also responsible for the renormalization of the electronic specific heat of a Fermi liquid at low-temperature. Using our previous very first estimate of Ω_p for LaO_{0.9}F_{0.1}FeAs [14], equation (2) has been used [13, 15] to consider a classical $el-ph$ scenario with $\lambda \sim 1.3$ for the high T_c -values and for a high-temperature saturation-like behaviour of the resistivity in the Pr based 1111-iron pnictides. However, the present improved knowledge and data do not provide support for such a point of view (see below). For more realistic estimates within a two-band model approach see reference [16].

Finally, Ω_p and λ determine also the pair-breaking parameter $\beta = \Omega_p^2\rho_0/8\pi(1+\lambda)T_{c0}$ for various unconventional pairing states [17, 18, 19, 20]:

$$-\ln\left(\frac{T_c}{T_{c0}}\right) = \psi\left(\frac{1}{2} + \frac{\beta T_{c0}}{2\pi T_c}\right) - \psi\left(\frac{1}{2}\right), \quad (3)$$

where $\psi(x)$ is the digamma function and T_{c0} denotes the transition temperature being at maximum in the clean-limit where the residual resistivity $\rho_0 \rightarrow 0$.

Here we report on the optical analysis of superconducting and nonsuperconducting parent compounds. Besides our own data also published data of other groups will be discussed and used in our analysis. We briefly introduce the employed codes for the determination of the electronic structure and the unscreened plasma frequencies, which we regard as quantities not affected by several possible many-body effects such as correlation, nonadiabatic, polaronic and polarization effects being under debate at present. With the aid of penetration depth data near $T = 0$ taken from μ SR (muon spin rotation (relaxation))-data we are in a position to estimate the total coupling strength between the charge carriers (both electrons and holes) and some still unspecified bosonic mode(s). The analysis of the background dielectric constant ϵ_∞ in the range of the

screened plasma frequency as derived from optical measurements sheds light onto the role played by correlation and polarization effects which is a central problem of general interest in modern solid state physics independently on the peculiar physics of high-temperature superconductivity.

2. Reflectivity and its analysis

2.1. Studies on polycrystalline $\text{LaO}_{1-x}\text{F}_x\text{FeAs}$ samples

Polycrystalline samples of $\text{LaO}_{0.9}\text{F}_{0.1}\text{FeAs}$ [21, 22] as well as of the undoped parent system LaOFeAs (also called (1111) compound) have been prepared as described in previous work [5, 23]. In general, the situation here parallels that for the HTSC. Right after their discovery, also only polycrystalline samples were available, and have been studied by reflectance measurements. Further, also the HTSC are quasi-2D metals with the highest plasma energy (PE) value for light polarization within the (a,b) crystal plane. In the case of HTSC, there is a number of publications devoted to polycrystalline pellets, exactly as in our studies of $\text{La}(\text{O},\text{F})\text{FeAs}$, which demonstrate that the reflectivity onset seen as a kink in the measured curves is a good measure of the in-plane PE value (see e.g. Kamaras K *et al.* [24]). Such studies already provided very important information on the optical properties of HTSC, e.g. they were used to study the doping dependence of the in-plane PE, and most importantly these results later on were corroborated by single crystal studies (see e.g. reference [25]).

For the optical measurements reported here the pellets have been polished to obtain appropriate surfaces. The reflectance measurements have been performed using a combination of Bruker IFS113v/IFS88 spectrometers. This allows us to determine the reflectivity from the far infrared up to the visible spectral region in an energy range from 0.009 up to 3 eV. The measurements have been carried out with different spectral resolutions depending on the energy range, these vary from 0.06 to 2 meV. Since the observed spectral features are significantly broader than these values, this slight variation in resolution does not impact our data analysis. All reflectance measurements were performed at $T = 300$ K.

In figure 1 we show the reflectance of our $\text{LaO}_{1-x}\text{F}_x\text{FeAs}$ samples ($x = 0, 0.1$). The reflectance significantly drops between 0.13 and 0.4 eV, thereafter it shows a small increase until about 0.6 eV before it starts to slightly decrease again. In addition, at about 2 eV another small upturn is visible for $\text{LaO}_{0.9}\text{F}_{0.1}\text{FeAs}$. We attribute the two small features at about 0.6 and 2 eV to weak electronic interband transition at the corresponding energies. This observation is in accord with the behavior of the optical conductivity $\sigma(\omega)$ predicted by Haule *et al.* [26] using dynamical mean-field theory (DMFT), where As 4p to Fe 3d interband transition slightly below 2 eV and a weak feature near 0.6 eV for the undoped parent compound LaOFeAs have been found. Again, our measurements on powder samples do not allow the extraction of their polarization. The steepest edge centered at about 250 meV with an high energy onset at about

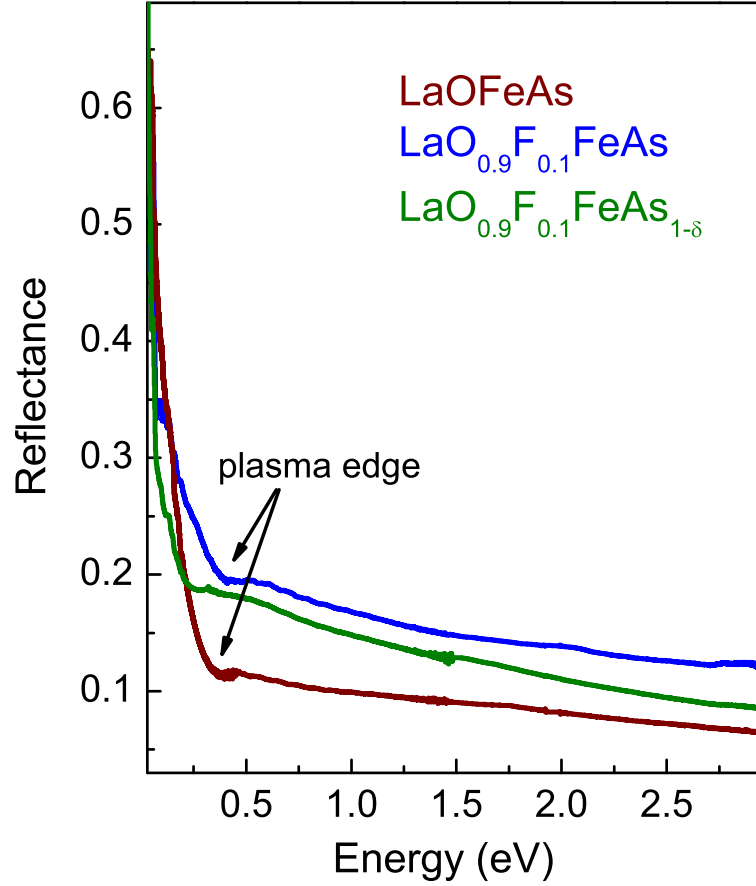


Figure 1. Reflectance of polished undoped LaOFeAs, optimally doped LaO_{0.9}F_{0.1}FeAs, as well as an arsenic-deficient sample LaO_{0.9}F_{0.1}FeAs_{1-δ} with $\delta \approx 0.1$. All three curves are characterized by a rather pronounced kink which is attributed to a plasma edge at about 380 meV and 395 meV, respectively. For the interpretation of the broad edge-like feature near 240 meV in the special case of LaO_{0.9}F_{0.1}FeAs_{1-δ} see figure 2 and text. In addition, there are signatures of interband excitations around 0.6 eV (and for LaO_{0.9}F_{0.1}FeAs at about 2 eV).

380(20) meV for LaOFeAs and 395(20) meV for LaO_{0.9}F_{0.1}FeAs represents the plasma edge or plasma energy, which is observed at relatively low values. In consideration of the quasi-2D character of the electronic states in LaO_{1-x}F_xFeAs and the expected strong anisotropy of the plasma energy for light polarized \parallel to the **(a,b)** and **c** crystal axes, respectively, the onset of the plasma edge in figure 1 gives a reasonable value of the in-plane value (i.e. for light polarized within the **(a,b)** crystal plane). Consequently, the in-plane plasma energies for the two LaO_{1-x}F_xFeAs samples (undoped and 10% electron doped) is almost independent of the doping levels studied here.

Within a simple Drude model, the value for the plasma energy allows a first, rather crude estimate of the charge carrier density in LaO_{1-x}F_xFeAs. Within this model, the observed screened plasma energy, ω_p , is given by $\omega_p^2 = 4\pi n e^2 / m \epsilon_\infty$, with n , e ,

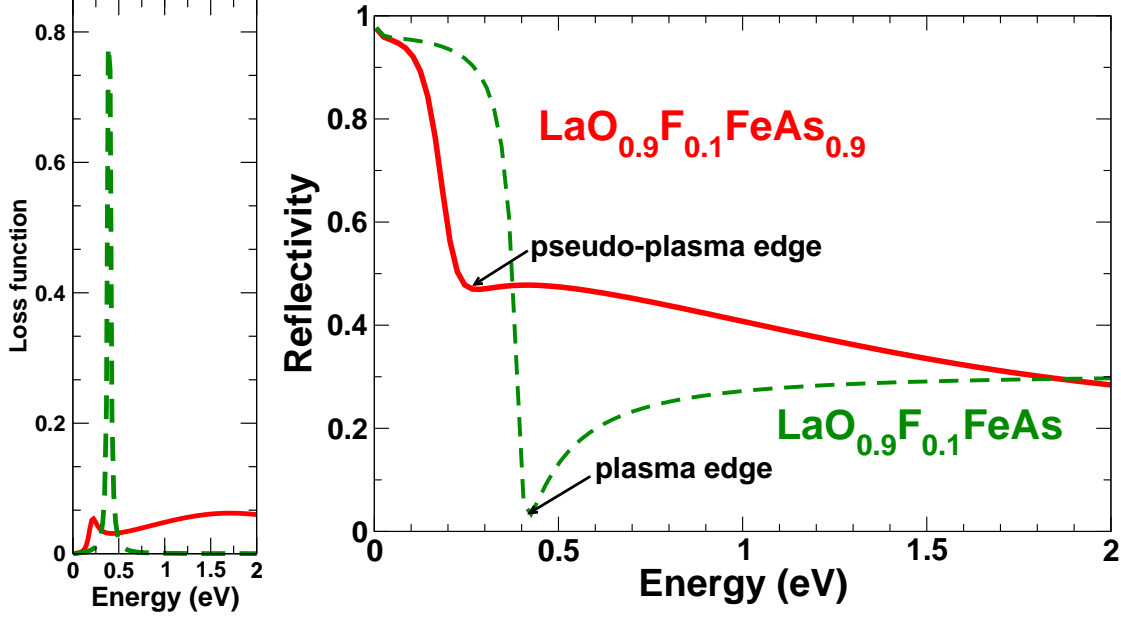


Figure 2. Idealized in-plane Drude-Lorentz model for the loss function (left) and the reflectivity (right) of optimally doped $\text{LaO}_{0.9}\text{F}_{0.1}\text{FeAs}$, as well as an arsenic-deficient sample $\text{LaO}_{0.9}\text{F}_{0.1}\text{FeAs}_{1-\delta}$ with $\delta \approx 0.1$. For a qualitative comparison with experimental polycrystalline data see figure 1. For fit parameters see text.

m , and ε_∞ representing the charge carrier density, the elementary charge, the effective mass of the charge carriers and the background dielectric screening due to higher lying electronic excitations [27]. Adopting an effective mass equal to the free electron mass, and $\varepsilon_\infty \sim 12$ [28], one would arrive at a rather low charge density of about $9 \cdot 10^{-20} \text{ cm}^{-3}$. We note, that this estimate ignores the strongly anisotropic nature of the electronic orbitals near the Fermi energy in $\text{LaO}_{1-x}\text{F}_x\text{FeAs}$. A more detailed discussion of the unscreened in-plane plasma energies found well above 1.3 eV but below 2 eV in all pnictide superconductors is given in the next sections see also table 2.

Finally, we examined also an arsenic-deficient sample $\text{LaO}_{0.9}\text{F}_{0.1}\text{FeAs}_{1-\delta}$ with $\delta \approx 0.1$ [22, 29]. Here at first glance a plasma-edge like feature near $\omega_p = 0.24 \text{ eV}$, only, would suggest that the screened plasma frequency is considerably lowered. (see figure 1). Adopting a linear scaling of the background polarizability $\varepsilon_\infty - 1$ with the As-concentration, one arrives at $\varepsilon_\infty \approx 10.5$ instead of 12 for the non-deficient sample. Within a nonlinear scaling suggested by the Clausius-Mossotti relationship between the dielectric constant and the ionic polarizabilities discussed in more detail in section 4.2 one estimates even a slightly smaller value of $\varepsilon_\infty \approx 9.97$. Thus, one would arrive at $\Omega_p = 0.79$ to 0.76 eV for the unscreened plasma frequency. However, such a strong change of Ω_p by about 0.6 eV (!) would imply very large changes in the electronic structure (e.g. by

filling the hole pockets and an additional mass enhancement) or alternatively a twice as large ε_∞ . Both scenarios are difficult to imagine microscopically. For this reason we will consider a third possible explanation with an almost unchanged Ω_p and a slightly reduced $\varepsilon_\infty \approx 10$. We ascribe the clearly changed optical properties to the presence of arsenic derived electrons and adopt that an absorption peak described by a Lorentzian curve like that absorption near 0.66 eV in the BaFe₂As₂ single crystal data with about 5% arsenic vacancies [30] (see below) might be mainly responsible for that unexpected feature. Simulating qualitatively the polycrystalline reflectance data shown in figure 1 by an effective Drude-Lorentz model we arrive at a corresponding Lorentzian curve peaked near 1.16 eV and a slightly lowered unscreened plasma frequency $\Omega_p = 1.3$ eV (A quantitative fit would require a more or less realistic account of the shapes of the microcrystalline grains and their anisotropic dielectric properties which, however, is without the scope of the present paper.). The oscillator strength of this Lorentzian-peak is expected to be about twice as large which is supported by our fit value of 6.5 eV, see figures 2-4 and compare table 1. The different binding energy might be related to the rather different As-environment in the 1111 and the 122 compounds with no La(O,F) layer in the latter and an enhanced pinning provided by the La³⁺ ions being close to the As-sites whereas in the former case it is provided by the less effective pinning due to Ba²⁺-ions. The resulting loss function and the optical conductivity are shown in figure 4. The obtained optical conductivity resembles the mid-infrared absorption observed by Yang *et al.* in a Ba_{0.55}K_{0.45}Fe₂As_{1- δ} single crystal [31, 30] with a $T_c \approx 30$ K slightly above our arsenic-deficient La-111 sample. This observation gives further support for our vacancy derived bound-electron scenario. In this context it would be interesting to study analogous effects in the related superconducting FeSe_{0.88} and other substoichiometric iron telluride and selenide compounds [32].

Here we would like to mention that a very small value for the unscreened plasma frequency has been derived from an ellipsometry study of LaO_{0.9}F_{0.1}FeAs and a subsequent analysis applying the effective medium approximation (EMA) to obtain $\sigma_{\text{eff}}(\omega)$ for a polycrystalline sample [28]. For spherical grains and $\sigma_{ab} \gg \sigma_c$ as expected for a quasi-2D metal (as is the case for LaO_{0.9}F_{0.1}FeAs), the EMA predicts $\sigma_{\text{eff}} \approx 0.5\sigma_{ab}$, which then would correspond to a slightly larger value of $\tilde{\Omega}_p^{ab} = 0.86$ eV. In addition some spectral weight from the Drude part was lost in reference [28] due to the fitting of broad Lorentzian-peaks also for the two low- ω interband transitions α_1 and α_2 at 0.75 and 1.15 eV, respectively. Adding this lost weight to the Drude term we arrive at an enhanced corrected Drude weight by a factor of 1.28 which corresponds to a corrected $\tilde{\Omega}_p^{ab} \approx 0.975$ eV. Moreover, since this value has been derived mainly from the low- ω , damped Drude region (below 25 meV), it is still renormalized by electron-boson coupling, and a high-energy boson well above 25 meV has been assumed to explain the high T_c at weak coupling. Using a weak total *electron-boson* coupling constant $\lambda \approx 0.61$ (see section 5.1) one estimates $\Omega_p = 1.24$ eV, close to a value of 1.37 eV suggested from the plasma energies in figure 1 and dielectric screening (see above).

2.2. BaFe₂As₂ single crystal studies

With the successful synthesis of single crystals, more detailed investigations of the optical response of iron pnictide superconductors become possible. In particular, the background dielectric constant ϵ_∞ can be determined more safely. Reflectivity data of Ba_{1-x}K_xFe₂As₂ and SrFe₂As₂ single crystals have been reported recently, and their analysis corroborates what has been derived from the polycrystalline samples as discussed above. In figure 3 we present reflectivity data of a BaFe₂As₂ single crystal and a light polarization within the (a,b) crystal plane. The investigated single crystal with the dimension of about 0.5x0.5x0.1 mm was grown from a tin flux. Elemental Ba, Fe, As were added to Sn in the ratio 1 : 2 : 2 : 15 and placed in a corundum crucible which was sealed in an argon filled silica ampoule. The sealed ampoule was heated in steps to 850°C with a rate of 20 K/h, hold for 36 hours and cooled down. The tin flux was removed by solving in diluted HCl. The resulting gray, crystals with metallic luster were washed in distilled water several times and finally dried.

The studied single crystal shows a thin platelet-like shape and a shiny (0, 0, 1) surface. The thorough characterizations via specific heat, resistivity, magnetic susceptibility and chemical composition analysis have been carried out on the crystals obtained from the same batch. Similar physical properties to those in the crystals reported in references [30] have been obtained. The EDX composition analysis of several specimens of this batch resulted an average composition of Ba_{0.95}Sn_{0.05}Fe₂As₂ and we expect $\sim 5\%$ Sn to be incorporated in the crystal structure. For the consequences of an As-deficiency with respect to low-frequency optical properties see below and for the upper critical field $B_{c2}(T)$ of the K-doped system see [29].

Also these data are characterized by a "kink"-like feature (but not by a sharp minimum as expected in the case of a clean single crystal!) in the reflectivity around 0.4 eV, with a steeper decrease at lower energy values. The polycrystalline samples as analyzed in the previous section did not allow a quantitative analysis of the reflectivity values due to relatively rough surfaces, but in the case of single crystal data as shown in figure 2 this is feasible, and figure 2 also shows a fit of our reflectivity data within a Drude-Lorentz model:

$$\epsilon(\omega) = \epsilon_\infty - \frac{\Omega_p^2}{\omega^2 + i\omega\Gamma_p} + \sum_{j=1}^3 \frac{\omega_{p,j}^2}{\omega_{0,j}^2 - \omega^2 - i\omega\gamma_j}. \quad (4)$$

This fit describes the data very well and allows the extraction of more physical information. The resulting fit parameters are summarized in table 1.

One important finding of our fit is the value for the screened plasma frequency $\omega_p = \Omega_p/\sqrt{\epsilon_\infty}$ of about 400 meV, which is in very good correspondence to what has been derived from the polycrystalline LaO_{1-x}F_xFeAs samples above. This demonstrates that this value is rather independent of the stoichiometry but is a characteristic feature of the FeAs planes common to all FeAs based superconductors. Furthermore, in order to obtain a reasonable description of our data within the Drude-Lorentz approach, it is necessary to include Lorentz oscillators above and *below* this unscreened plasma energy

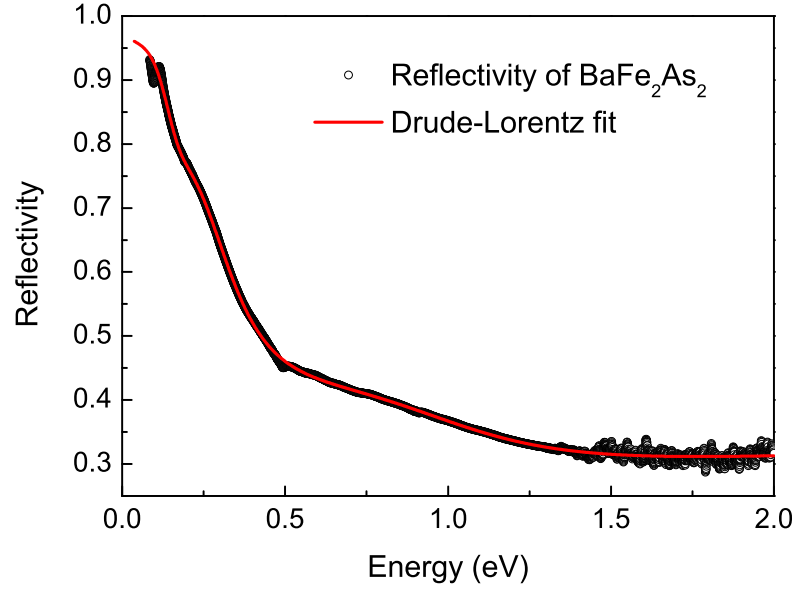


Figure 3. Reflectivity of a BaFe_2As_2 single crystal and a light polarization within the (a,b) crystal plane (open circles). The solid line represents the result of our Drude Lorentz analysis (see text).

(see table 1) at least for the BaFe_2As_2 (also called (122) compound), and other (122) systems.

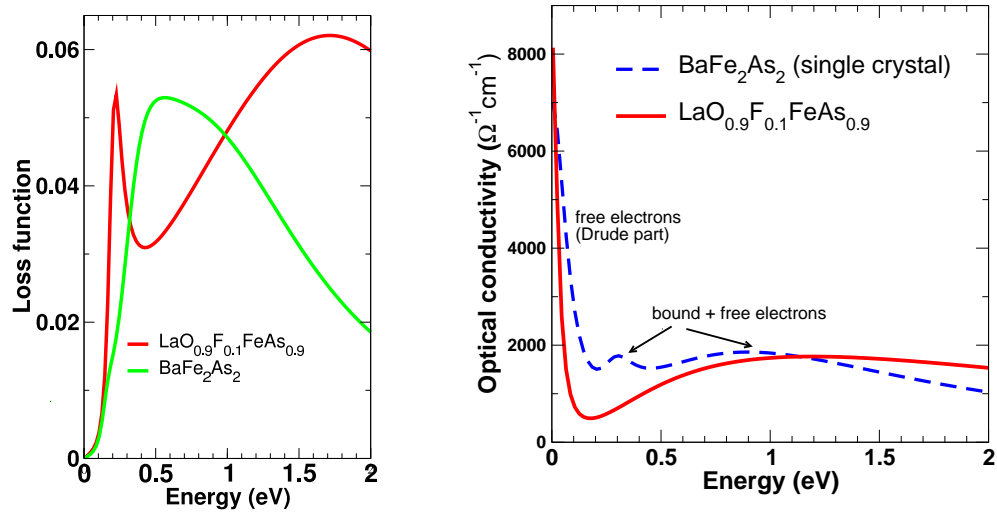


Figure 4. Experimental in-plane loss function (left) and optical conductivity (right) of a BaFe_2As_2 single crystal and the same for the suggested minimum Drude-Lorentz model for the arsenic-deficient La-1111 system. Adopting $\omega_{0,1}=1.16$ eV $\gamma_{0,1}=3.3$ eV and $\Omega_{p,1}=6.5$ eV for the "bound" electrons as well as $\Gamma_p=0.03$ eV and $\Omega_p=1.3$ eV for the free electrons for the latter. Compare table 1 and equation (4).

Table 1. Parameters derived from a Drude-Lorentz fit of the reflectivity of a BaFe₂As₂ single crystal. Here the following notation has been used: Ω_p = Drude plasma frequency, Γ = Drude width, $\omega_{0,j}$ = Lorentz oscillator position, γ_j = Lorentz oscillator width, $\omega_{p,j}$ = individual Lorentz plasma frequency (or oscillator strength), and ϵ_∞ = background dielectric constant).

j	$\omega_{0,j}(eV)$	γ_j (eV)	$\omega_{p,j}(eV)$	Γ_p (eV)	$\Omega_p(eV)$	ϵ_∞
1	0.2	0.16	0.79	0.031	1.58	14.9
2	0.66	2.9	4.31	0.087 [33]	1.6 [33]	
3	0.93	1.63	1.86			

Regarding the clean (1111) systems, so far clearly visible interband transitions have been observed only above the plasma edge [21, 28]. An inspection of the atomic occupancies given for such single crystals obtained from the Sn-flux by [30], reveals a non-negligible amount of disorder, first of all of arsenic-vacancies about half as large as in the polycrystalline arsenic-deficient sample reported above. For this reason we assume that the low-frequency Lorentzian-peaks describe in both cases transitions from As-vacancy introduced, more or less localized, states below the Fermi-level E_F but well above the usual As $4p$ states which occur about 2 eV below E_F . These states are thought to accommodate the large amount of electrons compared for instance with its free electron Hall number $n_H \approx 5 \cdot 10^{20} \text{cm}^{-3}$ [29]: $\approx c_{vac}Z/\tilde{v}_{cell} \approx 10^{21} \text{cm}^{-3}$ which would otherwise heavily overdope the La-1111 system or electron dope the nominal 122 parent compound, where $Z < 3$ is the effective anionic As-charge, $c_{vac} \approx 0.05$ to 0.1 denotes the atomic As-vacancy concentration and $v_{cell} = 70.75 \text{\AA}^3$ denotes the molar cell volume.

Although the reflectivity curves for FeAs based single crystals as presented in figure 3 and in the literature so far [31, 33, 34, 35, 36, 37] do not agree in all aspects, there are essential parameters in common, which give quite a lot of insight into the physics of these systems. First, interband excitations are present in the energy ranges around 0.2-0.3 eV and 0.6 - 2 eV which most likely arise from the manifold of iron related bands that cross the Fermi level [38]. Second, the background dielectric screening in the energy range of the plasma energy is quite large with values of about 12 to 16. Noteworthy, comparable values have been already observed occasionally also for other transition metal compounds [39]. Third, the value of the (unscreened) plasma frequency is in the range of 1.4 - 2 eV, rather independent of the doping level, and importantly, it is substantially smaller than what is predicted from density functional (DFT) based band structure calculations. The latter issue will be discussed in detail in the following sections.

3. FPLO analysis of the unscreened plasma frequency

The theoretical plasma frequencies have been taken from DFT based calculations in the local (spin) density approximation (L(S)DA). We used the full potential local orbital

code [40] in version 7 with the standard double numerical basis. The theoretical unscreened (Drude) plasma frequencies are derived from the Lindhard intra band expression Ω_p (see references [41, 42] for the isotropic case and equation (5) below for the straightforward anisotropic generalization). They basically represent the Fermi surface average of the Fermi velocity squared.

It has been checked that the results are converged within a few percent with respect to the k -integration scheme. We used the experimental lattice constants and the theoretical arsenic position. However, the frequencies seem not to be too sensitive to the lattice parameters. In the case of doped systems the simple virtual crystal approximation has been used. Thus, here we report calculations of the eigenvalues of the anisotropic conductivity (dielectric function) tensor

$$\hbar^2 \Omega_{pl,\alpha\alpha}^2 = 4\pi e^2 N(E_F) v_\alpha^2, \quad \alpha = x, y, z \quad (5)$$

where the Fermi velocity components v_α have been averaged over all Fermi surface sheets (FSS) and $N(E_F)$ denotes the total density of states at the Fermi level E_F for both spin directions. In the tetragonal phase the 'xx' and 'yy' component do coincide and we will then denote as in-plane plasma 'ab'-frequency whereas the out-of plane 'c'-plasma frequency is given by the 'zz' component. In terms of individual Fermi surface sheets (bands) equation (5) can be rewritten as

$$\Omega_{p,tot}^2 = \sum_i \Omega_{p,i}^2 \quad (6)$$

where i denotes the band index. In the pnictides under consideration all DFT-calculations predict up to five bands (FSS) at E_F consisting of electron (el) and hole (h) FSS. For the sake of simplicity the discussion of multiband effects all these FSS can be lumped into one effective el -FSS and one h -FSS, thus resulting in frequently used two-band models.

Due to the layered structure of the pnictides one has $\Omega_p^{ab} \gg \Omega_p^c$. The larger in-plane distance and the smaller transfer integrals in c -direction for the (1111) systems as compared for instance with the (122) systems is mainly responsible for the relative small values of both in-plane and out-of plane components. For comparison we included also calculations by Singh [43] for the case LaOFeP and Boeri *et al.* [44] for the case of LaOFeAs and LaOFeP where different bandstructure codes have been used. We note that different codes results in essentially the same unscreened plasma frequency. All are clearly a factor of 1.5 to 2 larger compared with the experimental values (see table 2), pointing to the presence of many-body effects which for instance may cause a mass renormalization. Several possibilities to resolve this issue will be discussed below.

The inspection of the calculated and empirically found unscreened plasma frequencies shows a very sensitive dependence on the Fe-Fe-distance which in the tetragonal phase is given by the in-plane lattice constant $a/\sqrt{2}$. Since $\Omega_p \propto v_F \propto t_{dd}a$, where t_{dd} is a representative value for the in-plane Fe-Fe $3d$ transfer integrals, a simple power-law has been predicted considering the related Slater-Koster integrals [45]. As a

Table 2. Comparison of calculated (DFT) and experimental unscreened in-plane (*ab*) plasma frequencies measured in eV for polycrystalline samples (PC) and single crystals (SC). For completeness, the theoretical out-of plane values are shown, too. In the references the first citations notation denotes the experimental optical data (if available) and the second one the structural data employed in the DFT calculations.

Compound	DFT (ab)	DFT (c)	Experiment (ab)	Sample	Reference
LaOFeAs	2.1 - 2.3	0.25-0.34	1.33	PC	present work
LaO _{0.9} F _{0.1} FeAs	2.1 - 2.3	0.25-0.34	1.36	PC	
LaO _{0.9} F _{0.1} FeAs	2.1 - 2.3	0.25-0.34	1.37	PC	[21]
”			0.6 (1.24)	PC	[28] see text
LaO _{0.1} F _{0.1} FeAs _{0.9}			≤ 1.3	PC	present work
SrFe ₂ As ₂	2.8	1.36	1.72	SC	[33]
La _x Sr _{1-x} Fe ₂ As ₂	2.8	1.36 - 1.46			
SrFe _{2-x} Co _x As ₂	2.7	1.35			
BaFe ₂ As ₂	2.63	0.8	1.72	SC	
”			1.6	SC	[33]
”			1.58	SC	present work
”			1.39	SC	[36]
K _x Ba _{1-x} Fe ₂ As ₂	2.63	0.8	1.5	SC	
K _{0.45} Ba _{0.55} Fe ₂ As ₂	2.63	1.72	1.9 ± 0.2	SC	[31]
CaFe ₂ As ₂	2.95	1.96			
LiFeAs	2.9	0.83			[46]
NaFeAs	2.68	1.16			[47]
LaOFeP	2.37	0.47	1.85	SC	[37]

result we expect

$$\Omega_p \approx \Omega_{p,0}/(a/a_0)^\nu, \quad (7)$$

where $a_0 = 4 \text{ \AA}$ has been introduced for convenience. According to Harrison [45] we adopt $\nu = 4$ and arrive at $\Omega_{p,0} = 1.4 \text{ eV}$. Applying the approximate expression (7) to rare earth-1111 systems, where to the best of our knowledge no high-frequency optical data are available, and considering for instance two superconductors with the highest transition temperatures $T_c > 50 \text{ K}$: SmO_{0.85}FeAs and NdO_{0.85}FeAs with $a = 3.897 \text{ \AA}$ and $a = 3.943 \text{ \AA}$ we estimate $\Omega_p = 1.55 \text{ eV}$ and 1.48 eV , respectively.

Having now a large enough set of available empirical plasma frequencies $\Omega_p \sim 1.4$ to 1.7 eV we are in a position to re-estimate the mentioned above transport coupling constants [13, 15]. With these values using equation (2) we would arrive, instead at $\lambda \sim \lambda_{tr} = 1.3$, at a *superstrong* coupling regime $\lambda \sim 4$ to 5 (!). Then we should have to ask, why is T_c of the iron pnictides so low? In our opinion other scattering mechanisms than the usual *el-ph* interaction, in the *el-el* or the *el-spin fluctuation* channels, contribute to $\rho(T)$ and possibly dominate it in the quasilinear region. Adopting a weak *el-ph*

coupling constant ~ 0.2 like the one estimated by Boeri *et al.* [44] a second linear region might be achieved beyond 600 K, only. To the best of our knowledge there are no experimental data available at present for that region.

4. Discussion of possible related many-body effects

4.1. The Mott-Hubbard scenario

Our LDA-FPLO band structure calculations for the nonmagnetic ground state of LaOFeAs provide a value for the plasma frequency within the (\mathbf{a}, \mathbf{b}) crystal plane of $\Omega_p^{LDA} = 2.1$ eV and a small value for a polarization along the \mathbf{c} axis of 0.34 eV in accord with 2.3 eV and 0.32 eV given in reference [44]. Note that these "bare" values do not describe the screening through ε_∞ caused by interband transitions. In order to get the measured values of $\omega_p = 0.395$ eV for the fluorine doped and 0.38 eV for the undoped parent system an unusually large value of $\varepsilon_\infty \sim 28.3$ to 33.9 would be required which seems to be unrealistic and instead intermediate values $\varepsilon_\infty \sim 12$ to 15 considerably larger than those for cuprates (4 to 6) would be expected [28]. Then, for the empirical unscreened plasma energy Ω_p a value about 1.4 eV would be expected on the basis of our reflectance data. Thus the question arises, what is the origin of these renormalizations? In view of the transition metal iron it is natural to consider moderate short range Coulomb interaction induced correlations as a possible reason. To get more insight into the role of possible correlation effects adopting the parameter set of Haule *et al.* [26] we calculated at first numerically the interband contribution to the complex dielectric function $\varepsilon(\omega)$ from the in-plane DMFT optical conductivity $\sigma(\omega)$ between 1 and 6 eV for the undoped LaOFeAs given in figure 5 of reference [26]. From its static value we obtained $\varepsilon_\infty = 5.4$, only (see figure 5). Taking into account the small differences in the optical spectra between the undoped LaOFeAs and the optimally doped LaO_{0.9}F_{0.1}FeAs as shown in sections 2 and 3, we will not distinguish between their ε_∞ -values in the following discussion. (Using the ionic polarizabilities of F⁻¹ and O⁻² given in section 4.2 and the unit cell volume of $v=142.32$ Å³ [1] for LaOFeAs, one estimates from equation (9) a slight change of its ε_∞ to 11.61 or 11.25 for the parameter sets of references [48, 49] and [50, 51, 52, 53, 54, 55], respectively, compared with 11.5 to 12 for LaO_{0.9}F_{0.1}FeAs [28].) In the strongly correlated (narrow band limit) limit $U_d \gg W$, for a very qualitative discussion, ε_∞ can be written approximately in the following way

$$\varepsilon_\infty = 1 + \frac{f_{pd}}{E_{pd}} + \frac{f_{dd}}{U_d} + \dots, \quad (8)$$

where $W \sim 2$ eV denotes the total Fe 3d bandwidth, $E_{pd} \sim 2$ eV is the oscillator strength for the arsenic-iron 4p-Fe3d interband transitions and f_{dd} describes the transitions through the Mott-gap. From our numerical simulations for $U_d = 4$ eV we estimate $f_{pd} = 4.6$ eV and $f_{dd} = 8.4$ eV. The resulting curve is shown in figure 8 (left).

Despite the crude estimate of equation 8 in the weak U -limit, in general for smaller values for the onsite Coulomb repulsion U_d within the DMFT-approach would result in

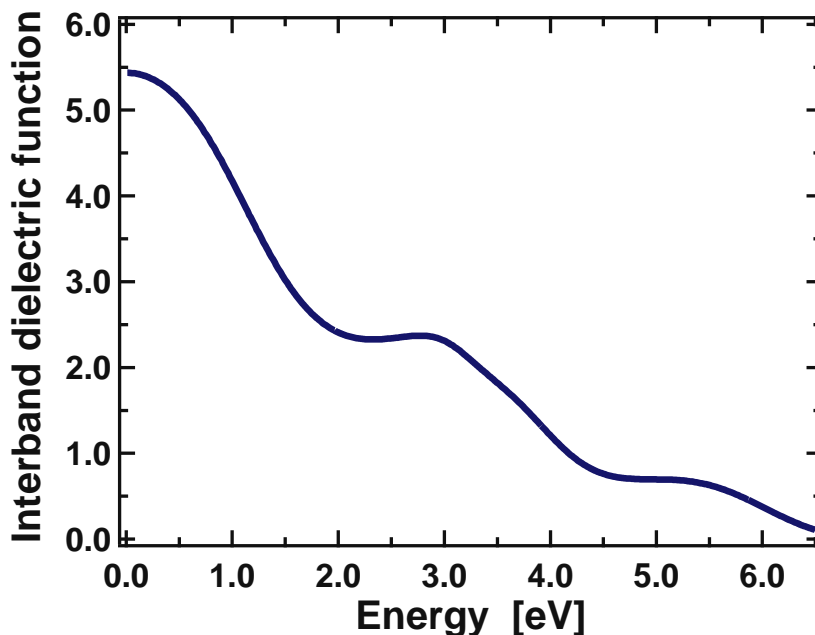


Figure 5. Interband contribution to the real part of the dielectric function $\varepsilon_1(\omega)$ of LaOFeAs using the DMFT-calculation for its $\sigma(\omega)$ as given by Haule *et al.* in reference [26] in figure 5 therein with $U_d = 4$ eV.

somewhat larger ε_∞ values due to an energy shift of the interband transition from the lower Hubbard band. Hence, a corresponding systematic DMFT study with sufficiently smaller U_d and J_d -values would be of interest. Alternatively to figure 6 (left) one might expect that for small U -values there should be no visible influence of U at all. Then a negative curvature instead of the positive curvature suggested by equation (8) might be realized. A corresponding guess taken from our previous paper [21] is shown in figure 6 (right). Anyhow, a more sophisticated study should shed light on the "screening" mechanism of the bare Coulomb repulsion. In this context it is noteworthy that the arsenic-polarization (solvation) mechanism proposed by Sawatzky *et al.* [11, 12] briefly discussed in the next subsection 5.1.2 seems to give a similar behaviour as equation (8) (see figure (7) (right)).

In contrast to Haule *et al.* [26], Anisimov and Shorikov *et al.* [56, 57] argue that LaOFeAs is in an intermediate U regime but strongly affected by the value of the Hund's rule exchange J_d . Hence, ε_∞ should be strongly increase and the adopted relatively strong Coulomb repulsion $U_d = 4$ eV is not compatible with the available optical data implying a much larger $\varepsilon_\infty > 10-15$. Thus, we are obliged to consider a weakly correlated scenario.

A somewhat similar attempt to describe the experimental reflectivity $R(\omega)$, a reduced plasma frequency and "bad metal" effects, i.e. strong damping effects (first considered by Haule [26] like in a marginal Fermi liquid) has been undertaken in a recent study by Laad *et al.* [58] using a simplified version of the dynamical mean-

field theory. Although at first glance a seemingly similar behaviour has been obtained, quantitatively the results are not very convincing because (i) using $U_d = 4$ eV and at the same time ignoring the hybridization with As $4p$ states reduces the minimal eight-band model to an effective five-band model where *reduced* effective Coulomb interactions and in particular also the onsite term U -values should be considerably reduced, (ii) the important screening by the background due to pd and other non- dd interband transition described implicitly also by ε_∞ in our approach has been ignored in calculating the reflectivity $R(\omega)$, (iii) a comparison with results from measurements on powder samples requires a proper treatment of the anisotropic grains, for instance, at least approximately within an effective medium theory.

4.2. The weakly correlated As-polarization scenario

Taking into account the criticism of strong on-site Coulomb repulsion U_d and Hund's rule coupling exchange J_d mentioned above, the recently proposed novel, quite interesting polarization (solvation) scenario [11] for the pnictide components As, Te, Se, or P as seen by the Fe $3d$ electrons is of special interest. In this context we will compare our empirical values of ε_∞ with the contribution of the polarizability from As alone, $\alpha_{\tilde{\text{As}}}$,

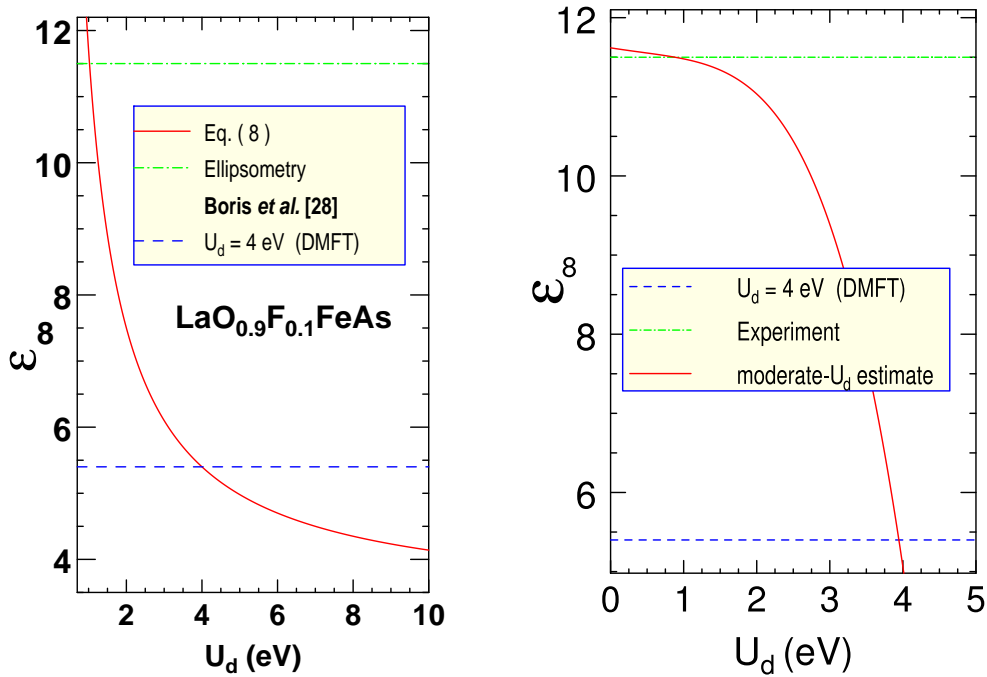


Figure 6. Semi-empirical relation between the total coupling constant from the mass enhancement entering the penetration depth *vs.* interband screening modeled by the dielectric background constant ε_∞ using equation (8)(left) and a first estimate proposed in reference [21] (right) (see also figure 7 (right)).

as adopted by Sawatzky *et al.* [11]. For this purpose to get a first rough estimate, we employ the well-known Clausius-Mossotti (also known as Lorenz-Lorentz relation) for the sake of simplicity ignoring anisotropic screening effects

$$\alpha_{tot} = \frac{v \varepsilon_{\infty} - 1}{b \varepsilon_{\infty} + 2}, \quad b = \frac{4\pi}{3} \quad \text{or} \quad \varepsilon_{\infty} = \frac{3}{1 - b\alpha_{tot}/(v)} - 2 > 1, \quad (9)$$

(Note that the Lorentz factor $b = 4\pi/3$ has been derived for the case of cubic symmetry.) Using for $\text{LaO}_{0.9}\text{F}_{0.1}\text{FeAs}$ $\varepsilon_{\infty}=12$ and $v = 140.5\text{\AA}^3$ with two As-sites per unit cell we arrive at $\alpha_{tot} = 26.35 \text{\AA}^3$ and $\tilde{\alpha}_{tot} = 13.17 \text{\AA}^3$ per As-site already close to 9 to 12 \AA^3 adopted by Sawatzky *et al.* [11]. For BaFe_2As_2 with $\varepsilon_{\infty}=14.9$, $v = 203.96\text{\AA}^3$ with four As sites per unit cell one obtains $\alpha_{tot} = 40.05 \text{\AA}^3$ which corresponds to $\tilde{\alpha}_{tot} = 10.01 \text{\AA}^3$ per As-site. Since the other atomic sites are expected also to contribute to $\tilde{\alpha}_{tot}$, we briefly consider their influence adopting the simple expression provided by the polarizability additivity rule [48]

$$\tilde{\alpha}_{As} = \left(\tilde{\alpha}_{tot} - \frac{1}{N_c} \sum_i \alpha_{\text{ion}_i} \right) / (1 - c_{\tilde{v},As}), \quad (10)$$

where the sum runs over all remaining ions(atoms), N_c is the number of As-sites per unit cell, and $c_{\tilde{v},As} \sim 0.1$ denotes the atomic concentration of As-vacancies. Then it is clear that these ignored ionic contributions may somewhat change our empirical estimates of the dominant As-contribution we are mainly interested in. In fact, adopting for the contribution of Ba^{2+} 1.7\AA^3 and -1.0\AA^3 for that of Fe^{2+} [50, 55] one arrives at a slightly larger value for $\tilde{\alpha}_{As} \approx 10.32 \text{\AA}^3$, and a smaller value of $\tilde{\alpha}_{As^{3-}} \approx 7.89 \text{\AA}^3$ is obtained using instead the parameters $\alpha_{\text{Fe}^{2+}} = 1.339 \text{\AA}^3$ and $\alpha_{\text{Ba}^{2+}} = 1.57$ as recommended in reference [48]. Taking into account the presence of As-vacancies in the order of 5% atomic percent [30] a lower value of $\tilde{\alpha}_{As^{3-}} \approx 8.3 \text{\AA}^3$ is obtained.

For the former case of $\text{LaO}_{0.9}\text{F}_{0.1}\text{FeAs}$ we estimated these corrections due the presence of other ions, too. Using the following values for their polarizabilities [52]: 1.13\AA^3 for La^{3+} , 2.68 for O^{2-} , 3\AA^3 for F^- [50], and again -1\AA^3 for Fe^{2+} [50]. As a result we finally arrive at an empirical value of $\tilde{\alpha}_{As^{3-}} = 10.49 \text{\AA}^3$. But using again the empirical polarizabilities recommended by Shannon and Fischer [48] with $\alpha_{\text{O}^{2-}}^0 = 1.988 \text{\AA}^3$ and $\alpha_{\text{F}^-}^0 = 1.295 \text{\AA}^3$ one arrives at $\tilde{\alpha}_{As^{3-}} = 8.74 \text{\AA}^3$. Thus, also for this different set the As-polarizabilities of two different materials are large and close to each other [49]. Thus, the empirical numbers derived from our reflectivity data are in excellent agreement with $\alpha_{As} \approx 10 \text{\AA}^3$ suggested by Sawatzky *et al.* [11], if the ionic polarizations of all ions are taken into account.

Next, LaOFeP could be used to understand the role of polarization effects comparing the ε_{∞} with those of the La-1111 based arsenic compounds with sufficiently higher superconducting and magnetic transition temperatures, except the parent compound itself. Since the corresponding fit parameters except the unscreened plasma frequency were not shown in reference [37] we are restricted to a qualitative discussion. From the reflectivity data shown in figure 1 of reference [37] one might ascribe the local minimum in between 4000 and 5000 cm^{-1} , (i.e. around 0.5 eV) to the plasma

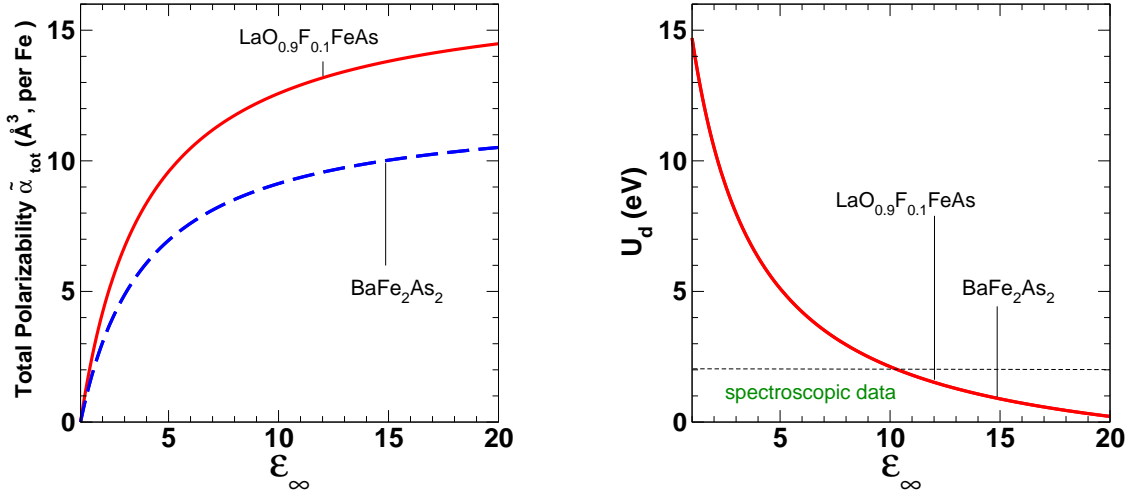


Figure 7. Total polarizabilities from equation (9) (left). Schematical view of the "screened" on-site Coulomb repulsion U_d of Fe 3d states (the so called Hubbard U) vs. background dielectric constant (right). For the bare case we adopted $U_0 = 14.7$ eV [67]. The stripe denotes the region of U_d estimated by various electron spectroscopy methods [68, 69]

edge but then one would arrive at a larger or close ϵ_∞ for LaOFeP compared with the arsenic counterpiece. Therefore we suggest that the actual plasma edge is masked by an interband transition or by a P-vacancy induced absorption like from the As-vacancies in two of the above considered arsenide systems. In fact, for a sequence of polarizability differences $\tilde{\alpha}_{As} - \tilde{\alpha}_P = 0, 1, 2, 3 \text{ \AA}^3$ we estimate (predict) from equation (9) $\epsilon_{\infty,P} = 14.4, 10.2, 7.7, 6.1$, respectively. Then the plasma edge would be near 0.487 eV, 0.58 eV, 0.67 eV, 0.75 eV, where $\epsilon_{\infty,As} = 11.5$ and $v_P = 133.75 \text{ \AA}^3$ have been used. In addition we have assumed that the polarizabilities of the other ions La^{3-} , O^{2-} , and Fe^{2+} remain unchanged, i.e. they cancel out in the difference $\tilde{\alpha}_{As} - \tilde{\alpha}_P$. A P-vacancy scenario might also explain the suppression of an antiferromagnetically ordered state in favour of superconductivity as observed in LaOFeP below 6K. If indeed $\epsilon_{\infty,P}$ is sufficiently smaller than 11 to 15 found here for two arsenide compounds, we would predict also a somewhat larger U_d value for LAOFeP. Both predictions can be checked experimentally.

To get some insight in the accuracy of equation (9) and to check the polarizability of the next important most competing ionic component O we considered the cuprates La_2CuO_4 and Li_2CuO_2 in the same way using in addition 0.2 \AA^3 for the polarizability of Cu^{2+} and 0.0286 \AA^3 for Li^+ summing up all ionic polarizabilities one obtains $\alpha_{tot} = 24.28 \text{ \AA}^3$ and 11.31 \AA^3 , respectively, (both with two formula units per unit cell). As a result with unit cell volumes of $v = 187.89 \text{ \AA}^3$ and $v = 98.42 \text{ \AA}^3$ realistic ϵ_∞ -values of 4.54 and 3.74, respectively, are obtained from equation (9). Using the set of polarizabilities proposed by Shannon and Fischer [48] $\alpha_{\text{O}^{2-}}^0 = 1.988 \text{ \AA}^3$, and $\alpha_{\text{Cu}^{2+}} = 1.23 \text{ \AA}^3$, we arrive at $\alpha_{tot}^0 = 10.524 \text{ \AA}^3$ and $\epsilon_\infty^0 = 3.434$ in the free ionic

approximation [59]. The analysis of the loss function $-\text{Im}[1/\varepsilon(\omega)]$ for Li_2CuO_2 within the framework of a five-band $\text{Cu}3d\text{-O}2p$ extended Hubbard model [60] reveals with $\varepsilon_\infty = 3.6$ a very close value. The calculated ionic charges $Q_{\text{Cu}} = 1.797e$ and $Q_{\text{O}} = -1.972e$ are also very close to the idealized ionic picture with values of $2e$ and $-2e$, respectively.

In the cuprates the background dielectric constant ε_∞ is dominated by the polarizability of O^{2-} , i.e. by the $2p$ -component similarly as in our case by the As $4p$ states. Anyhow, in spite of the surprisingly good description in both cases more sophisticated calculations beyond the isotropic cubic approximation used in deriving equation (9) are nevertheless highly desirable [61, 62] in view of the importance of the polarization problem for the elucidation of the mechanism of superconductivity in the iron pnictides. In this context we would like to note that our estimated empirical values of $\alpha_{\text{As}} < 12\text{\AA}^3$ are probably not large enough to ensure a bipolaronic formation at low temperature, i.e. a Bose condensation-like scenario of superconductivity in the iron based pnictides such as proposed by Sawatzky *et al.* [11, 12] This objection is also supported by the observation of a nearly linear temperature dependence of the upper critical field near T_c instead of an expected pronounced positive curvature generic for bipolarons $B_{c2}(T) \propto (T_c - T)^{1.5}$ [10], the Pauli-limiting behaviour observed in some cases [22, 29] as well as the clear observation of Fermi surface related features such as the de Haas van Alphen (dHvA) effect in LaOFeP [63] and last but not least the numerous angle resolved photoemission experiments (ARPES) [64, 65]. Anyhow, our conclusions about unstable bipolarons should be taken with some cautions in view of the approximate character of equation (9) and the fact that our estimated polarizabilities are determined from optical frequencies around the screened plasma frequencies whereas the dielectric polarizabilities entering the original Clausius-Mossotti equation are determined usually in the range of kHz-10 MHz and include both ionic and electronic components. The extrapolation of our results to that quasi-static limit even below typical phonon-frequencies remains an open and interesting question worth to be considered in future. We admit that such ionic effects (or lattice effects in general) might support the electronic polarization effects and favour finally the formation of bipolarons, too. However, even when bipolarons are stabilized it is unclear what will their mass? Too heavy bipolarons is a general serious problem for most bipolaronic scenarios to explain rather high- T_c values. Another possibility would be also the so-called boson-fermion scenario (or s -channel scenario) where real bipolarons occur not as prepaired pairs already above T_c but occur only below T_c where they coexist with Cooper pairs (see e.g. reference [66] and references therein).

In order to illustrate the polarization effect on the Coulomb repulsion on Fe sites we consider again the relationship between U_d and ε_∞ employing equation (9). According to reference [11] the actual on-site Coulomb repulsion U_d in a multiband Hubbard-model (for the sake of simplicity we ignore slight differences between the various involved five Fe $3d$ -orbitals) is given by the difference

$$U_d = U_0 - 2E_p, \quad E_p \sim 0.5 \sum_i E_i^2, \quad (11)$$

where the polarization energy E_p reflects the electric field produced at all surrounding polarizable sites due to the additional charge related to the on-site double occupancy and U_0 is the bare Coulomb repulsion for which we adopt 14.7 eV [67]. In the point charge approximation one has $E_p = \sum \tilde{\alpha}_{ji}e^2/R_{ij}^4$ resulting in $2\tilde{\alpha}e^2/R_{Fe,As}^4 = 0.868\tilde{\alpha}/[\text{\AA}^3]$ eV in the nearest neighbour (NN) approximation ignoring the influence of other ions, where $R_{Fe,As} \approx 2.4 \text{ \AA}$ denotes the NN arsenic-iron distance. Instead of taking into account also the dipole-dipole interaction and summing up all contributions within a single FeAs layer as it was done in reference [11] in the point charge approximation, we simply assume that the polarization energy E_p scales linearly with α where the constant of proportionality u_1 has been determined from the condition to reproduce approximately our DMFT based result of $\varepsilon_\infty = 5.4$ for $U = 4$ eV given in the previous subsection 4.1. Using equations (9) and (11) the resulting phenomenological curve shown in figure 7 (right) reads

$$U_d = U_0 - u_1 \frac{3\tilde{v}(\varepsilon_\infty - 1)}{4\pi(\varepsilon_\infty + 2)}, \quad (12)$$

where \tilde{v} denotes the volume per iron site. This way we arrive at $U_d \approx 1.5$ eV for $\text{LaO}_{0.9}\text{F}_{0.1}\text{FeAs}$ and $U \approx 1$ eV for BaFe_2As_2 using the same DMFT based coefficient u_1 also for the latter compound. Thus, our estimated U_d values are in both cases *smaller* than the total band width $W \sim 2$ eV. Taking into account the quasi-degeneracy of all five Fe 3d orbitals involved one comes to the conclusion that repulsive correlation effects should play a minor role except maybe for the magnetic exchange interaction affected by the superexchange and the Hund's rule couplings as well. The same reduced size of the on-site Coulomb repulsion has been estimated based on various electron spectroscopy measurements [68, 69]. Note that residual Coulomb interactions of $U_{eff} = 320$ to 380 meV and a Hund's rule coupling $J_{eff} = 70$ meV have been used for instance by Korshunov and Eremin [70, 71] within a four-band theory for the description of thermodynamic properties related to the nesting derived spin density wave (antiferromagnetic) ground state and its magnetic excitations of the undoped parent compound LAOFeAs and other the iron pnictides (We remind the reader that the extended Hubbard model including besides all five Fe 3d also the As 4p orbitals is a 16-band model.) Without doubt our estimated strongly reduced $U_d \sim 1$ eV-values might be helpful to understand microscopically the low value of the former, especially, if a reduced, but yet sizable, value of the NN intersite Fe-Fe Coulomb interaction V is taken into account: $U_{eff} \sim U - V$, provided a repulsive $V > 0$ is still obeyed in contrast to an expected *attractive* $V < 0$ adopted within the bipolaronic scenario of Sawatzky *et al.*, where the polarization $\tilde{\alpha}_{As} \geq 12 \text{\AA}^3$ is so strong to change its sign, i.e. V would be over-screened. In addition, U_{eff} is also reduced in the process of mapping down the 16-band model "integrating out" the As-4p states [56] exhibiting a moderate hybridization with the Fe 3d states. Anyhow, the extremely small value of J_{eff} compared with expected 0.7 to 1 eV remains as a puzzle to be resolved. (Since $2J$ is given as the difference of the both onsite (intra-atomic) U and the intra-atomic-interorbital U' and to first approximation both are expected to be reduced in the same way by the polarization of the surrounding

ions.). Possibly, the explicit account of an additional direct ferromagnetic exchange interaction K_{pd} might be helpful to resolve this puzzle. $K_{pd} \sim 200$ meV was introduced for the two dimensional corner-shared cuprates by Hybertsen *et al.* [72]. For instance, in almost all edge-shared cuprates such as the above mentioned Li_2CuO_2 or in $\text{Li}_2\text{ZrCuO}_4$ [74] with Cu-O-Cu bond angles near 90° (just like as the Fe-As-Fe bond angle in the iron pnictides considered here) K_{pd} amounts about 50 to 80 meV [60, 74]. There K_{pd} is decisive for the observed ferromagnetic NN-exchange interaction being much more important than the ferromagnetic coupling provided by the Hund's rule coupling J_p on the intermediate oxygen O $2p$ orbitals. The reason for that is that K_{pd} affects the total exchange already in the second order of the perturbational theory whereas the Hund's rule J_p coupling appears only in fourth order (four small pd transfer integrals) [73].

Also a negative U -scenario as proposed in reference [75] to solve the puzzle of the too large calculated magnetic moment in the framework of LDA+ U seems to be unlikely. According to our estimate $\varepsilon_\infty > 25$ would be required (see figure 7). Anyhow, a detailed comparison with other metallic compounds which exhibit large ε -values would be interesting also in view of searching for new superconducting compounds and for systems with other exotic ground states.

First estimates of the corresponding polaronic effect result in mass renormalization by a factor of 2 in accord with our findings for Ω_p and those from ARPES data for 122 superconductors [64] and de Haas van Alphen studies for LaOFeP [63]. Thus, the mentioned above strongly reduced Coulomb repulsion U_d can be understood based on empirical considerations for the ionic polarizabilities and is in accord with empirical findings analyzing various electron spectroscopy data [68, 69, 56].

5. The *el-boson* coupling strength and constraints for pairing mechanisms

Naturally, the most interesting problem of the pnictide superconductivity is the elucidation of its mechanism. At the present relatively poor knowledge and still not very high sample quality (with respect to impurities and other defects) reflected for instance by the high residual resistivities ρ_0 and an unknown mesoscopic structure due to a pronounced tendency to an electronically driven phase separation [76, 77] at least for the (122)-family, a comprehensive theoretical description is impossible. In such a situation one may adopt various simplified scenarios (with increasing complexity) and look for qualitative checks like bipolaron condensation vs. Cooper pair formation, the symmetry of the order parameter(s), the coupling strength and the effect of disorder in order to discriminate at least a part of the huge amount of already proposed scenarios.

5.1. One-band Eliashberg analysis

We start with the simplest possible version of an effective single-band theory where the formation of a condensate of Cooper pairs is assumed. (The case of prepared bipolarons

can be excluded by the nearly linear T -dependence of the upper critical field near T_c (see Fuchs *et al.* [22, 29].) Here the mass of the paired charge carriers is affected by the virtual retarded interaction with collective excitations (bosons) being present in any solid. The corresponding $el-el$ interaction may be attractive or repulsive, supporting or weakening a specific type (symmetry) of pairing in addition to the unretarded Coulomb interaction which may be also repulsive or attractive under special circumstances [16]. Thus, from the standard Eliashberg-theory applied to the case of type-II superconductor with weak or intermediately strong coupling ($\lambda \leq 2$)[78] one obtains for the penetration depth $\lambda_L(0)$ at zero temperature using convenient units

$$\sqrt{\varepsilon_\infty}\omega_p[\text{eV}]\frac{\lambda_L(0)[\text{nm}]}{197.3\text{nm}} = \sqrt{(n/n_s(0))(1 + \lambda_{tot}(0))(1 + \delta)}, \quad (13)$$

where $\lambda_L(0)[\text{nm}]$ is the experimental (a, b)-plane penetration depth extrapolated to $T = 0$. $\Omega_p = \sqrt{\varepsilon_\infty}\omega_p$ denotes the empirical unscreened plasma frequency shown in table 2, $n_s(0)$ is the density of electrons in the condensate at $T = 0$ and n denotes the total electron density of all conduction bands which contribute to the unscreened Ω_p , and δ is the disorder parameter

$$\delta = 0.7\frac{\gamma_{imp}}{2\Delta(0)} \equiv 0.7\frac{\gamma_{imp}}{RT_c} \approx \frac{\gamma_{imp}}{5T_c}, \quad (14)$$

which is small but finite even in the quasi-clean limit. R denotes the gap-to T_c ratio $R = 2\Delta(0)/T_c$ which in moderately strong coupled superconductors slightly exceeds the BCS-value $R_{BCS} = 3.52$. Notice that all three factors, the strong coupling correction described by the mass enhancement factor $Z = 1 + \lambda$, the disorder $D = 1 + \delta$, as well as the condensate occupation parameter $N = n/n_s$ under the root obey the inequality ≥ 1 . Let us note that the possibility to extract the el -boson-coupling constant from a comparison of the high frequency optical response with the renormalized low-energy plasma frequency which determines the superfluid density has been proposed (in the clean-limit $D \equiv 1$ and for the BCS case $N = 1$) already in 1987 by Gurvitch and Fiory [79] and again in 1992 by Hirsch and Marsiglio [80]. But to the best of our knowledge there were no systematic applications to real superconductors. A first step in this direction is presented in subsections 5.1.1 and 5.1.2. Note that equation (13) can be generalized taking into account two unusual situations which, however, may be present for certain pnictides as discussed below in subsection 5.1.2 in the context of LaOFeP [37] in more detail: (i) some residual mass renormalization is still present at room temperature in the frequency region of the screened plasma energy ~ 0.4 to 0.5 eV i.e. $\lambda(\omega = \omega_p, T = 300 \text{ K})$ is not very small. This may happen when the spectral density of the coupled boson extends to very high-frequencies and (ii) the superconductivity is somewhat suppressed due to fluctuations of a competing neighbouring (e.g. magnetically ordered) phase. To take these effects into account we may write:

$$Z = \frac{1 + \lambda_{tot}(0)}{1 + \lambda_{tot}(\omega_p, T)}, \text{ or } \lambda_{tot}(0) = \frac{Z - 1}{1 - r}, \text{ where } r = \frac{\lambda_{tot}(\omega_p, T)}{\lambda_{tot}(0)}, \quad (15)$$

and

$$D = (1 + \delta)(1 + f), \quad (16)$$

where $f \geq 0$ is a phenomenological parameter which measures the fluctuational influence of all competing phases. The latter effect occurs beyond the standard mean-field approximation and a for a treatment of all instabilities (various superconducting phases with different symmetry of the order parameter (s, s^\pm, p, d -waves), SDW's, ferromagnetism, and CDW's, etc.) on equal footing. Since such a corresponding comprehensive microscopic theory is not available at present, f has to be treated as a phenomenological parameter.

In classical BCS-type superconductors at $T = 0$ all quasiparticles participate in the superfluid condensate, i.e. $N = 1$. In complex multicomponent superconductors like underdoped cuprates the possibility of $n_s < n$ has been discussed by several authors (see e.g. Rüfenacht *et al.* [81]). In the present case it might also happen in the case of coexisting CDW or SDW ordering with superconductivity as observed for instance in transition metal dichalcogenides such as NbSe₂ or in clean magnetic borocarbides (HoNi₂B₂C). The well-known classical superconductor Nb which much stimulated the development of the strong coupling theory provides an almost ideal possibility to illustrate the power of equation (13). Adopting $N = 1$ we may examine the case of very clean samples with resistivity ratios RRR up to $\sim 2 \cdot 10^4$ (!)[84] for which a small disorder parameter δ is expected. In fact, with $\lambda_L(0) = 31.5$ nm [82], 32 nm [83], 34.3 nm [84], 35 nm [85] and the calculated LDA-value of $\Omega_p = 9.24$ eV [86] or the empirical value of 9.2 eV [85] and $\lambda = 1.12$, $T_c = 9.22$ K [87] one arrives at $\delta = 0.026$, 0.059 and 0.217, respectively, which point to a very clean-limit regime. In fact, using the experimental gap to T_c ratios of 4.1 [83, 88] and 3.79 [84] these δ -values correspond very small scattering rates of 1.4 K, 3.2 K, and 10.8 K, respectively, only. Based on these results we will denote a regime with $\delta < 1$ as a quasi-clean limit.

Turning back to LaO_{0.9}F_{0.1}FeAs we adopt also the BCS relation $n=n_s$ and $\delta \approx 0.93$ being still in the quasi-clean limit at $T = 0$. Then, using $\varepsilon_\infty = 12$ [28] and $\lambda_L(0) = 254$ nm [5] or 242 nm [89] one estimates $\lambda_{tot} \sim 0.6$ and 0.45, respectively, i.e. the superconductivity is in a weak coupling regime for our samples with a bulk $T_c = 26$ K (according to the μ SR-data [5] while the resistivity yields a slightly larger value of 27-28 K).

The effect of the dielectric background constant renormalized by both the disorder and the actual condensate density $\varepsilon^* = \varepsilon_\infty/DN$ on the coupling strength is shown in figure 8. Note that a substantial impurity scattering absent in the quasi-clean limit would further reduce λ_{tot} . We note once more that our empirical $\Omega_p \approx 1.36$ eV differs from the LDA-prediction of 2.1 eV for the nonmagnetic ground state within the LSDA.

5.1.1. Comparison with other pnictide superconductors In the present context it is interesting to apply our analysis also to other iron based pnictide superconductors for which the penetration depth is known. Khasanov *et al.* [90] reported μ SR measurements for the related FeSe_{0.85} system with a relative low $T_c = 8.26$ K (probably related to the smaller polarizability of Se compared with As). They found from their μ SR-data a penetration depth $\lambda_L(0) = 406$ nm. Adopting a typical plasma frequency of about

1.3 to 1.5 eV (compare table 2), one arrives at $ZDN \approx 7.16$ to 9.53. For a weak to intermediately strong *el-boson* coupling strength $\lambda_{tot} = 0.5$ to 1 one is left with a relatively large factor $DN \geq 3.58$ to 4.76 i.e. either the system under consideration is strongly disordered or affected also by fluctuations of a competing phase (see equation (16)). Alternatively this factor is enhanced due-to $N > 1$, i.e. the condensate density n_s is much smaller than the total electron density n . Finally, Li *et al.* [34] studying $\text{Ba}_{0.6}\text{K}_{0.4}\text{Fe}_2\text{As}_2$ ($T_c = 37$ K) reported $\lambda_L(0) = 200 \pm 8$ nm adopting a dirty limit scenario in order to describe the observation of a gap in their reflectivity measurements. Then, in fact, adopting a relatively large value of $\Omega_p \approx 1.8$ to 2.1 eV such as suggested in reference [31] for the closely related system $\text{Ba}_{0.55}\text{K}_{0.45}\text{Fe}_2\text{As}_2$ one estimates from equation (13) $ZDN = 3.28$ to 4.47 and there is room for some disorder for weak to intermediately strong coupling $Z \sim 1.6$ to 2 provided $N = 1$.

The most interesting from the disorder and high-field properties point of view is the closely related system given by the arsenic-deficient compound $\text{LaO}_{0.9}\text{F}_{0.1}\text{FeAs}_{1-\delta}$ with improved superconducting properties near $T_c \approx 28$ K [22, 29]. The analysis of the Pauli limiting (PL) behavior for the closely related $\text{LaO}_{0.9}\text{F}_{0.1}\text{FeAs}_{1-\delta}$ system yields a similar value $\lambda \approx 0.6$ to 0.7 as derived from the Eliashberg-theory corrections to the BCS (called often “strong-coupling” corrections even for small or moderate values of λ) for its PL field $B_P(0) = 102$ T [22, 29]. Quite interestingly, the observed kink in the electron dispersion in the ARPES data by Wray *et al.* [91] for the 122 $(\text{Sr,Ba})_{1-x}(\text{K,Na})_x\text{Fe}_2\text{As}_2$ can be described with an effective $\lambda \gtrsim 0.6$ of the same order as that found for the La-1111-system [21] and adopted above for the corresponding rare earth system (see figure 9) and discussed in more detail there.

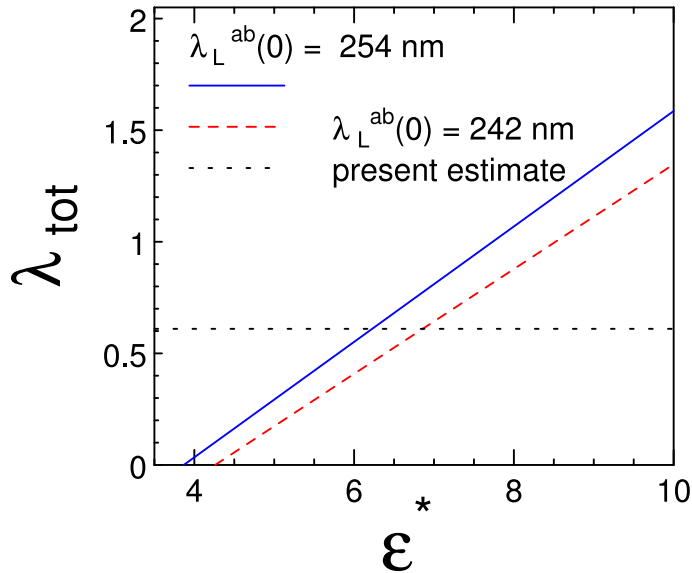


Figure 8. Empirical relation between the total coupling constant from the mass enhancement entering the penetration depth $\lambda_L(0)$ vs polarizability related renormalized dielectric background constant ϵ^* . The in-plane penetration depth values $\lambda_L^{ab}(0)$ have been taken from references [5, 89].

In spite of relatively large error bars it is noteworthy that an Uemura-plot type relation between the superconducting transition temperature and the squared of the empirical *unscreened* plasma energy Ω_p seems to hold (see figure 9) although the 1111-pnictides occur on *another* curve than the 122-pnictide superconductors [8]. The 1111-pnictides are more or less close to the hole-doped cuprates on an almost linear curve but with an additional negative constant. At present it is unclear what does this phenomenological result imply? Is there a critical carrier concentration necessary for the occurrence of superconductivity at variance with the Uemura-plot prediction? Or does it mean that for the present crystal structure types (1111, 122, and 111) very low carrier phases are simply not realized for chemical reasons and the vanishing T_c near $\Omega_p \sim 1$ eV is caused by other reasons *not* directly related to the carrier density? In the La-1111-family the smallest Ω_p occurs just near the phase boundary to the SDW-phase.

The 122-systems can be described by another linear relation but also with a negative constant. Note that the stoichiometric compounds LAOFeP [37] and NaFeAs[47] occur far from these two curves for the 1111 and 122 As-based families Further experimental and theoretical work is required to settle these points. A solution might be also helpful to understand better the mechanism of superconductivity in iron based pnictide superconductors. In the context of a (possibly) somewhat smaller ε_∞ and also a larger U_d for LaOFeP, its lower $T_c = 6$ K as compared with values of 18 K for LiFeAs or 26 K for LaO_{1-x}F_xFeAs might be a relevant hint for the elucidation of the still unknown mechanism of superconductivity in Fe pnictides, too.

The measured in-plane penetration depths of two LiFeAs powder samples with superconducting transition temperatures $T_c = 16$ and 12 K, respectively, amount $\lambda(0) = 195$ nm and 244 nm [7]. Since to the best of our knowledge optical data are still not available we estimate $\Omega_p = 1.77$ eV using equation (7) and the reported lattice constant $a = 3.77$ Å. The isostructural NaFeAs exhibits a larger lattice constant $a = 3.947$ and a lower $T_c = 9$ K [47].

LAOFeP deserves special attention due to its unusual properties and the relatively large amount of experimental single crystal data available for a phenomenological comprehensive analysis [37, 92, 93]. The penetration depth exhibits a quasi-linear temperature dependence pointing to unconventional superconductivity with nodes in the order parameter [92] which points possibly to a different superconducting phase compared with the nodeless FeAs based superconductors. From the measured in-plane penetration depth $\lambda_L(0) = 240$ to 250 nm [92] and $\Omega_p = 1.85$ eV we estimate a large value for $ZDN \approx 5.06$. Ignoring the possibility of $N > 1$ and adopting $\lambda_{tot} \leq 1$ as suggested by the dHvA-data [63] and ARPES data [95], one is left with $D \sim 2.5$ to 3.4. Since the measurements were performed on very clean single crystals [92] a large disorder parameter alone seems to be not very likely to explain the data. Instead we assume a sizable contribution of *fluctuations* measured by our phenomenological parameter f (see equation (16)) which is thought to be caused by the presence of at least one competing superconducting and/or magnetic phase(s). In this context we note that the possibility of enhanced penetration depths due to the vicinity of fluctuating magnetic phases have

been assumed very recently also in reference [94]. Finally, we note that the unsaturated temperature dependence of the optical mass renormalization shown in the inset of figure 3 (panel b) in reference [37] points to a residual $\lambda(\omega = \omega_p, T = 300\text{K})$ introduced in equation (15) which might be caused by a very broad spectral density (Eliashberg function) $\alpha(\omega)F(\omega)$ with non-negligible high energy contributions. Adopting $r(300\text{K}) = 0.25$ to 0.33 would be helpful to reduce the differences of mass renormalization as seen in optical data ($\lambda \approx 0.5$) compared with dHvA [63] and ARPES data [95] pointing to $\lambda \approx 1$. The account of r in Z would further increase D and the phenomenological fluctuation parameter f . If such an effect would be present also in other pnictide superconductors, our estimated coupling constants would be enhanced to $\lambda_{tot} \sim 1$.

Anyhow, whether the quantity Ω_p is related in fact to the superfluid density n_s remains unclear. Due to some similarity with the original Uemura-plot one might conclude that all free charge carriers are in the condensate and the renormalization by the *el-boson* interaction should be rather similar. Then the only free parameter within a single band approach is the disorder parameter δ . In this approach the rare earth 1111 compounds with the highest T_c -values ~ 40 to 56 K exhibit also the weakest disorder. For instance, adopting the same $\lambda_{tot} = 0.61$ as for $\text{LaO}_{0.9}\text{F}_{0.1}\text{FeAs}$ discussed above we take into account the increase of Ω_p due to the shortening of a as modelled by equation (7) and arrive at $\delta \approx 0.5$. This is a clear indication for the presence of multiband effects. Finally, disorder affects mainly that band with the slow particles to which the penetration depth λ_L is not very sensitive (see below). Finally, we note that in the related nickel arsenide $\text{LaO}_{0.9}\text{F}_{0.1}\text{NiAs}$ a coupling constant of $\lambda \approx 0.93$ has been found from a single-band Eliashberg analysis of its thermodynamic properties [35].

5.1.2. Comparison with other exotic superconductors Finally, it is interesting to compare our results for the Fermi surface averaged total coupling constant λ_{tot} of the Fe-pnictides given above with a similar analysis for other more or less exotic superconductors where the symmetry of the order parameter may be unconventional and in addition to phonons also other bosons such as crystal field excitations and/or spin fluctuations may play a crucial role.

Let us start with extended *s*-wave superconductors with intermediately strong *el-ph* coupling $\lambda_{el-ph} \sim 1$ for which the necessary experimental data is available (a corresponding comparison with LDA-based bandstructure calculation will be given elsewhere). We start with

(i) the nonmagnetic borocarbide $\text{YNi}_2\text{B}_2\text{C}$ ($T_c = 15.6$ K). According to Widder *et al.* [96] one has $\tilde{\Omega}_p = 4.25$ eV for the plasma frequency already renormalized by the *el-ph* interaction and $\lambda_{opt} = 1.2$ in accord with the Fermi surface averaged $\lambda = 1.05$ from specific heat data [97]. Using the penetration depth $\lambda_L(0) \approx \lambda_L(T = 3\text{K}) = 58$ nm from the μSR data by Ohishi *et al.* [98], one arrives at $(1 + \delta) = 1.56$. Hence, a quasi-clean limit value such as $\delta \approx 0.7$ estimated from the low-temperature optical data of Bommeli *et al.* [99] yields $\lambda_{tot} \approx 0.92$ rather close to the value of 1.05 derived from specific heat data mentioned above. Similarly using $\Omega_p = 6.01$ eV and $\delta = 0.7$ [99] one arrives at

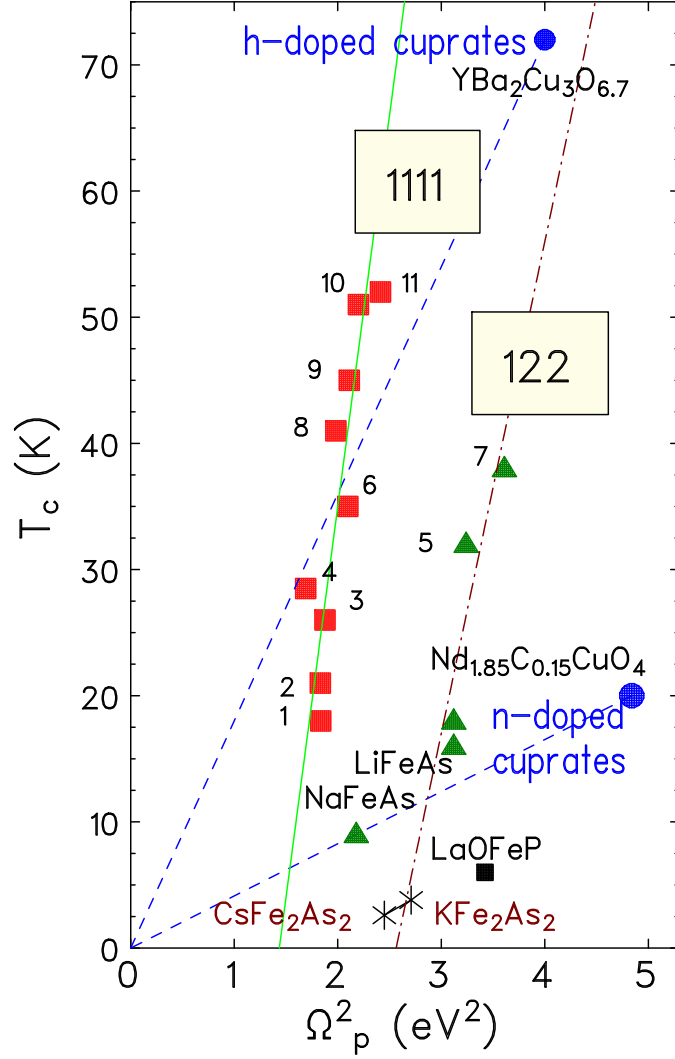


Figure 9. Uemura-plot type relation between the superconducting transition temperature T_c and the empirical squared unscreened plasma frequency *not renormalized* by the *el-boson* interaction as derived from optical and μ SR measurements for selected Fe-pnictide superconductors. The shown materials are $\text{LaO}_{1-x}\text{F}_x\text{FeAs}$ (1- $x=0.06$ [8], 2- $x=0.075$ [5] 3- $x=0.1$ [21]) 4- $\text{LaO}_{0.9}\text{F}_{0.1}\text{FeAs}_{0.9}$ (present work), 5- $\text{Ba}_{0.55}\text{K}_{0.45}\text{Fe}_2\text{As}_2$ [31], 6 - $\text{Ba}_{0.6}\text{K}_{0.4}\text{Fe}_2\text{As}_2$ [8], 7 - $\text{CeO}_{0.84}\text{FF}_{0.16}\text{FeAs}$ [4], 8- $\text{NdO}_{0.88}\text{F}_{0.12}\text{FeAs}$ [4] 9 - $\text{Sm}_{0.82}\text{F}_{0.18}\text{FeAs}$ [89], 10- $\text{NdO}_{0.85}\text{FeAs}$ [6] 11 - $\text{SmO}_{0.85}\text{FeAs}$ [6]. The points 7-11 and LiFeAs are predictions extrapolated from equation (7) using the actual lattice constant a .

$\lambda = 0.996$ even still closer to the specific heat value. Next, let us consider

(ii) a typical A15-superconductor, namely, V_3Si ($T_c = 17$ K). Here $\lambda_L(0) \approx$

$\lambda_L(T = 3.8\text{K}) = 108$ nm derived from μSR measurements by Sonier *et al.* [100]. The experimental plasma frequency of $\Omega_{pl} = 2.8 \pm 0.2$ eV [42, 101] has been obtained from room-temperature infrared data in between 0.16 and 0.62 eV using a pure Drude-model relation according to it the slope $1/(1 - \epsilon_1)$ vs ω^2 is given by $(\Omega_p/\hbar)^{-2}$. But this means that no ϵ_∞ has been taken into account. Hence an Ω_p obtained this way actually represents a *screened* plasma frequency and the real unscreened plasma frequency must be larger. For this reason one obtains too small disorder parameters δ if one adopts for total coupling *el-boson* constant $\lambda_{tot} = 0.9$ obtained from an Eliashberg-theory analysis of its thermodynamic properties [102] based on tunneling data for the spectral density $\alpha^2F(\omega)$ [103]. This procedure is the most accurate way to determine the relevant coupling strength for a standard superconductor. Then using the above mentioned penetration depth one would have $(1 + \lambda)(1 + \delta) = 2.026, 2.35$ to 2.7 , i.e. $\delta = 0.026, 0.24$ to 0.42 for the lower bound, the mean value and the upper bound, respectively. Thus it is clear why the lower bound is unrealistic. We may refine this way $\Omega_p = 2.9 \pm 0.1$. Then one is left with a ratio of 1.15 between $\Omega_{p,LDA} = 3.35$ eV and the refined experimental value. This ratio is a bit smaller than ~ 2 found for the pnictide superconductors considered above. Another phonon mediated superconductor with a sizable *el-ph* coupling is

(iii) MgCNi_3 for which $\lambda \approx 1.8$ has been found and $\Omega_{p,LDA} = 3.17$ eV has been calculated applying the mentioned above FPLO-code [78]. According to table 2, and according to our general experience for empirical plasma frequencies, one has $\Omega_p \approx (2/3)\Omega_{p,LDA}$. Thus we adopt $\Omega_p = 2.1$ eV. Using the measured penetration depth of $\lambda_T(0) = 231.5$ nm [104] one arrives at $DZ = 6.07$ substituting our empirical strong coupling value $\lambda = 1.8$ we are left with a relative small disorder parameter $\delta = 1.17 \sim 1$ in accord with our previous assignment of a quasi-clean limit regime in this compound [78].

(iv) The $\text{Ba}_{1-x}\text{K}_x\text{BiO}_3$ ($T_c \approx 30$ at optimal doping) exhibits a penetration depth of $\lambda_L(0) = 198.5$ nm [105] and $\lambda = 1.4$ has been estimated by Zhao [105]. With an unscreened plasma frequency of $\Omega_{pl} = 2.9$ to 3 eV [106, 107] one arrives at relatively large values $\delta \approx 2.55$ to 3.25 , where in the last case $\lambda \approx \lambda_{tr} \approx 1$ suggest by Nagata *et al.* from the high- T resistivity data using equation (2) has been suggested. In other words $\text{Ba}_{1-x}\text{K}_x\text{BiO}_3$ is a dirty strongly coupled superconductor.

Turning (v) to the heavy fermion superconductor $\text{PrOs}_4\text{Sn}_{12}$ ($T_c = 1.85$ K) and to its non- $4f$ counter part $\text{LaOs}_4\text{Sn}_{12}$ ($T_c = 0.74$ K). Their penetration depths amount $\lambda_L(0) = 353.4$ nm and 470 nm, respectively. To the best of our knowledge there are no optical data available. But theoretical calculation predict very strongly coupled superconductivity with $\lambda \approx 3.3$ in the former case and weakly coupled superconductivity with $\lambda \approx 0.3$ in the last case [108]. Here the strong coupling contribution is expected due to nonphononic quadropolar crystal field excitations. If this picture is correct, one might predict lower bounds for the unscreened plasma frequency: $\Omega_p > 1.16$ eV in the former case and 0.479 eV in the latter case. Finally, turning to cuprates, we consider first

(vi) the hole (under)doped HTSC $\text{YBa}_2\text{Cu}_3\text{O}_{6.67}$ with $\lambda_L(0) = 178.4$ nm (see figure 6 of reference [109]) and $\Omega_p \approx 2$ eV one arrives at $(1+\lambda)(1+\delta) = 3.27$, i.e. strong coupling $\lambda_{tot} \sim 2$ in the quasi-clean limit regime which is in nice accord with the ARPES data of the underdoped $\text{YBa}_2\text{Cu}_3\text{O}_{6.6}$ system where $\lambda_{tot} = 1.59$ has been derived from a kink in the dispersion-laws of the quasiparticles [110] and it was described by the authors mainly to interaction with the magnetic resonance mode. We close this subsection considering

(vii) the electron-doped $\text{Nd}_{1.85}\text{Ce}_{0.15}\text{CuO}_{4-\delta}$ where the screened plasma frequency derived from the peak of the loss function amounts about 1.06 eV and the plasma edge (minimum) in the reflectivity data occurs near 1.3 eV [111]. The volume of the unit cell amounts $v = 188.7 \text{ \AA}^3$ [112]. Using the ionic polarizabilities like those mentioned in subsection 4.2 we arrive at an unscreened value of Ω_p in between 2.2 and 2.7 eV. Using equation (9) we estimate $\varepsilon_\infty \approx 4.51$ and this way $2.25 \text{ eV} \leq \Omega_p \leq 2.76 \text{ eV}$. Anlage *et al.* [83] measured $\lambda_L(0) = 105 \pm 20 \text{ \AA}$. Whereas Luke *et al.* found in μSR measurements $\lambda_L(0) = 230$ nm. Then we finally estimate $\lambda_{tot}(0) \leq 1$ for this cuprate with a $T_c \approx 20$ K, only. Our estimated coupling constant λ_{tot} is in accord with a recent theoretical estimate of 0.7 by Cappelutti *et al.* [113] based on the Holstein- t - J model and of 0.8 by Park *et al.* [114] based on an analysis of their ARPES data. Hence, electron-doped cuprates exhibit a similar behaviour as LiFeAs and NaFeAs with respect to the relation of T_c and the unscreened plasma frequency (see figure 9) and with respect to the *el-boson* coupling constant with La-1111 iron based superconductors.

5.2. Multiband effects

Let us consider the simplest case of two effective bands, where for instance one band could stand for the two electron bands and the second band for the two hole bands predicted by the DFT-LDA calculations mentioned above. Rewriting the total unscreened plasma frequency of equation (6) as

$$\Omega_{p,tot}^2 = \Omega_1^2 + \Omega_2^2 \equiv \Omega_1^2 (1 + \beta^2), \quad (17)$$

where $\beta = \Omega_2/\Omega_1$ and the index ‘p’ has been omitted, one obtains the following straightforward generalization of equation (13) (compare also the two-band expressions for the penetration depth as given in references [115, 116]):

$$\Omega_1 \lambda_L(0) = \sqrt{\frac{Z_1 D_1 N_1}{1 + \beta^2 \frac{Z_1 D_1 N_1}{Z_2 D_2 N_2}}}, \quad (18)$$

where Z_α denotes the mass enhancement factor of the band $\alpha = 1, 2$. $Z_\alpha = 1 + \lambda_\alpha$ with the total coupling constant (i.e. summed up over all interacting *el-boson* channels) including also the interband scattering, $N_\alpha = n_\alpha/n_{\alpha,s}$ is the inverse relative condensate occupation number of the band α and $D_\alpha = 1 + \delta_\alpha$ is the corresponding disorder parameter generalizing equation (14). For coinciding coupling constants and disorder parameters, i.e. $\lambda_1 = \lambda_2$ and $\delta_1 = \delta_2$, the one-band picture with its weak or moderate coupling strength discussed above is reproduced (see figures 8 and 10). Upon weakening (strengthening) the coupling in one band say, in band 1, stronger (weaker) couplings are

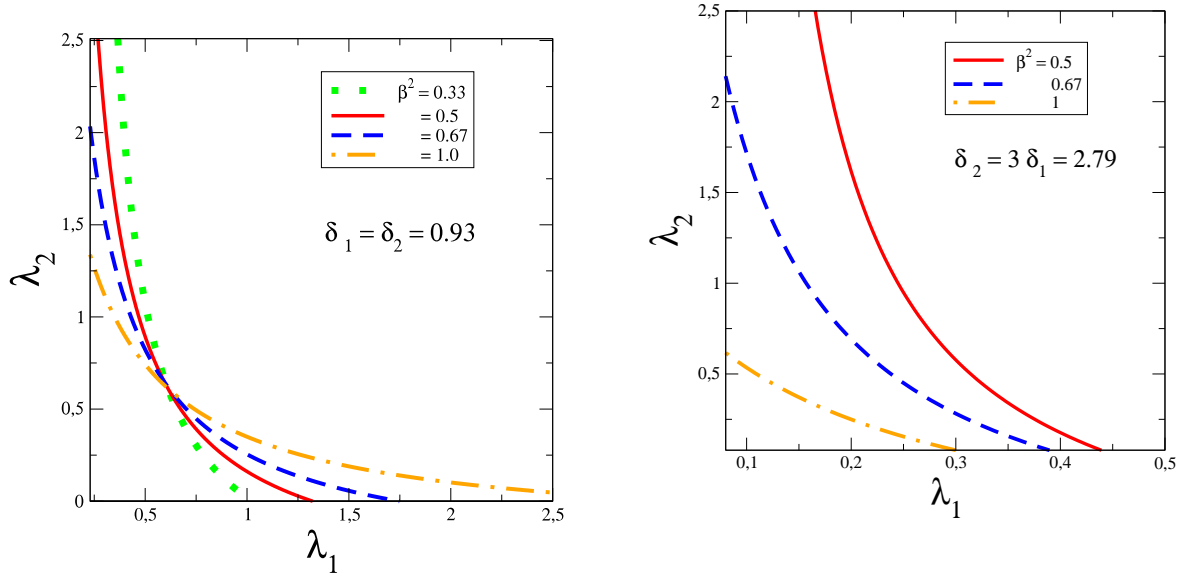


Figure 10. Constraint for the *el*-boson coupling constants λ_1 and λ_2 for various individual Drude plasma frequencies measured by the parameter $\beta = \Omega_2/\Omega_1$ using the experimental value of the penetration depth $\lambda_L(0) = 254$ nm [5] and the empirical total unscreened plasma frequency $\Omega_p = 1.37$ eV [21] for $\text{LaO}_{0.9}\text{F}_{0.1}\text{FeAs}$ (left) the same for enhanced disorder in the “slow” band 2 (right).

introduced in band 2. Naturally, the band with the larger coupling exhibits the larger gap, if the corresponding couplings support the actual pairing state which, however, has not been specified in our approach. From that constraint there is, in principle, taking into account the present poor knowledge of parameters no practical bound for λ_2 , i.e. for the band with the slower quasi-particles, whereas the coupling constant λ_1 for the band with the faster charge carriers is restricted from below and from above as well. At the upper bound $\lambda_2 = 0$, whereas it formally diverges at the lower bound, provided $\lambda_1^{\min} > 0$. In the special case when $\beta^2 \ll 1$, i.e. of a light and a heavy band, the fast electrons may mask the heavy electrons. For the iron pnictides under consideration the hole bands do exhibit somewhat smaller Fermi velocities (and also plasma energies) according to band structure calculations. Therefore one might ascribe our effective band 2 to these hole pockets. In general, we regard equation (18) as potentially helpful to identify the location of the larger and the smaller gap values in addition to other methods. A strongly coupled superconducting heavy subgroup which would be responsible for very high upper critical fields might be this way hidden by weakly coupled fast electrons.

6. Conclusion

We performed a combined theoretical and experimental study of the screened and unscreened in-plane plasma frequencies of iron based pnictide superconductors. The obtained moderate renormalization of the corresponding optical masses is similar the

one found frequently for other transition metals and is probably a normal Fermi liquid effect which gives strong support for the relevance of the electronic structure as calculated by various density functional based methods. Evidence for the presence of weak correlation effects can be deduced also from the obtained large background dielectric constants, exceeding 11, which is ascribed to the large polarizability α_{As} . A comparison with zero temperature penetration depth data from muon spin rotation data provides a new constraint for the total coupling strength of the *el-boson* interaction, the strength of impurity scattering rates and the density of quasi-particles involved in the superconducting condensate. This information yields also reasonable estimates for other more or less exotic superconductors.

Acknowledgments

We thank Eschrig H, Mazin II, Koitzsch A, Borisenko SG, Shulga SV, Singh D, Dolgov O, Kulić M, Eremin I, Craco L, Luetkens H, Plakida NM, Pickett WE, Timusk T, Maple B, Wang NL, van den Brink J, and Gvozdkov V for discussions concerning various points of the present work and the DFG (DR 269/3-1 (S.-L.D), (M.K), the SFB 463 (S.-L.D, G.F., and H.R.) and its Emmy-Noether Programme (H.R.)) and the ASCR project AVOZ10100520 (J.M.) for financial support.

References

- [1] Kamihara Y, Watanabe T, Hirano M, and Hosono H 2008 *J. Am. Chem. Soc.* **130** 3296
- [2] Uemura YJ 2008 *arXiv:0811.1546*
- [3] Goko T, Aczel AA, Baggio-Saitovitch, Bud'ko SL, Canfield PC, Carlo JP, Chen GF, Dai P, Hamann AC, Hu WZ, Kageyama H, Luke GM, Luo JL, Nachumi B, Ni N, Reznik D, Sanchez-Candela DR, Savici AT, Sikes KJ, Wang NL, Wiebe CR, Williams TJ, Yamamoto T, Yu W, and Uemura YJ 2008 *arXiv:0808.1425*
- [4] Carlo JP, Uemura YJ, Goko T, MacDougall GJ, Rodriguez JA, Yu W, Luke GM, Dai P, Shannon N, Myasaka S, Suzuki S, Tajima S, Chen GF, Hu WZ, Luo JL, and Wang NL 2008 *arXiv:0805.2186*
- [5] Luetkens H, Klauss H-H, Khasanov R, Amato A, Klingeler R, Hellmann I, Leps N, Kondrat A, Hess C, Köhler A, Behr G, Werner J, and Büchner 2008 *Phys. Rev. Lett.* **101** 097009
- [6] Khasanov R, Luetkens H, Amato A, Klauss H-H, Ren Z-A, Yang J, Lu W, and Zhao Z-X 2008 *Phys. Rev. B* **78** 092506
- [7] Pratt FL, Baker PJ, Blundell SJ, Lancaster T, Lewtas HJ, Adamson P, Pitcher MJ, Parker DR, and Clarke SJ 2008 *arXiv:0810.0973*
- [8] Hiraiishi M, Kadono R, Takeshita S, Myazaki M, Koda A, Okabe H, and Akimitsu J 2008 *arXiv:0812.2069v2*
- [9] Ren C, Wang Z-S, Luo H-Q, Yang H, Shan L, and Wen H-H 2008 *Phys. Rev. Lett.* **101**257006
- [10] Alexandrov AS 2004 *Physica C* **404** 22
- [11] Sawatzky GA, Elfmov IS, van den Brink J, and Zaanen , 2008 *arXiv:0808.1390*
- [12] Berciu M, Elfmov I, and Sawatzky GA 2008 *arXiv:0811.0214*
- [13] Bhoi D, Mandal P, and Choudhury P 2008 *Supercond. Sci. Technol.* **21** 125021
- [14] Drechsler S-L 2008 *et al. arXiv:0805.1321v1*. For an improved estimate using a more realistic larger value of the background dielectric constant ϵ_∞ as given in the present paper, see reference [21].
- [15] Sadovskii MV 2008 *Uspekhi Physics* **178** 1243; *arXiv:0812.0302*
- [16] Kulić M, Drechsler S-L, and Dolgov OV 2008 *arXiv:0811.3119.v2*; submitted to *Europhys. Lett.*

- [17] Lin J-Y *et al.* 1999 *Phys. Rev. B* **59** 6047
- [18] Petrovic C *et al.* 2002 *ibid.* **66** 054534
- [19] Mackenzie AP *et al.* 1998 *Phys. Rev. Lett.* **80** 161
- [20] Radtke RJ *et al.* 1993 *Phys. Rev. B* **48** 653
- [21] Drechsler S-L, Grobosch M, Koepernik K, Behr G, Köhler A, Werner J, Kondrat A, Leps N, Hess C, Klingeler R, Schuster R, Büchner B, and Knupfer M 2008 *Phys. Rev. Lett.* **101** 257004
- [22] Fuchs G, Drechsler S-L, Kozlova N, Behr G, Köhler A, Werner K, Nenkov K, Klingeler R, Hamann-Borrero J, Hess C, Kondrat A, Grobosch M, Narduzzo A, Knupfer M, Freudenberger J, Büchner B, and Schultz L 2008 *Phys. Rev. Lett.* **101**, 237003
- [23] Zhu X *et al.* 2008 *Supercond. Sci. Technol.* **21**, 105001
- [24] Kamaras K *et al.* 1987 *Phys. Rev. B* **59** 919
- [25] Basov D and Timusk T 2005 *Rev. Mod. Phys.* **77** 721
- [26] Haule K, Shim JH, and Kotliar G 2008 *Phys. Rev. Lett.* **100** 226402
- [27] Wooten F 1972 *Optical Properties of Solids*, (New York: Academic Press)
- [28] Boris AV, Kovaleva NN, Seo SSA, Kim JS, Popovich P, Matiks Y, Kremer RK, and Keimer B 2009 *Phys. Rev. Lett.* **102** 027001
- [29] Fuchs G, Drechsler S-L, *et al.* 2009 this volume.
- [30] Ni N, Bud'ko SL, Kreyssig A, Nandi S, Rustan GE, Goldman AI, Gupta S, Corbett JD, Kracher A, and Canfield PC 2008 *arXiv:0807.1040v1*; 2008 *Phys. Rev. B* **78** 014507
- [31] Yang J, Hübner D, Nagel U, Room T, Ni N, Canfield PC, Bud'ko SL, Carbotte JP, and Timusk T 2008 *arXiv:0807*
- [32] Lee K-W, Pardo V, and Pickett WE 2008 *Phys. Rev. B* **78** 174502
- [33] Hu WZ, Dong J, Li G, Li Z, Zheng P, Chen Gf, Luo JL, and Wang NL 2008 *Phys. Rev. Lett.* **101** 257005
- [34] Li G, Hu WZ, Dong J, Li Z, Zheng P, Chen GF, Luo JL, and Wang NL 2008 *Phys. Rev. Lett.* **101** 107004
- [35] Li Z, Chen GF, Dong J, Li G, Hu WZ, Wu D, Su SK, Zheng P, Xiang T, Wang NL, and Luo JL 2008 *Phys. Rev. B* **78** 060504
- [36] Pfuner F, Analytis JG, Chu J-H, Fisher IR, and Degeorgi 2008 *arXiv:0811.2195v1*
- [37] Qazilbash MM, Hamlin JJ, Baumbach RE, Maple MB, and Basov DN 2008 *arXiv:0808.3748v1*
- [38] Singh D and Du M 2008 *Phys. Rev. Lett.* **100** 237003
- [39] Nava F, Tu NK, Thomas O, Senateur JP, Madar R, Borghesi A, Gizeti G, Gottlieb U, Laborde O, and Bisi O 1993 *Mat. Science Rep.* **9** 141
- [40] Koepernik K and Eschrig H 1999 *Phys. Rev. B* **59** 1743; 2007 *Techn. Rep.* <http://www.fplo.de>
- [41] Cohen MH 1958 *Philos. Mag.* **3** 762
- [42] Mattheiss LF, Testardi LR, Yao WW 1978 *Phys. Rev. B* **17** 4640
- [43] Singh D 2008 *private communication*
- [44] Boeri L, Dolgov OV, and Golubov AA 2008 *Phys. Rev. Lett.* **101**, 026403
- [45] Harrison WA 1980 *Electronic Structure and Properties of Solids* (San Francisco: Freeman H and Company)
- [46] Tapp J, Tang Z, Lv B Samal K, Lorenz B, Chu CW, and Guloy AM 2008 *Phys. Rev. B* **78** 060505(R)
- [47] Parker D, Pitcher J, and Clarke SJ 2008 *arXiv:0810.3214*
- [48] Shannon RD and Fischer RX 2006 *Phys. Rev. B* **73** 235111
- [49] But using for fixed other parameters instead of $\alpha_{\text{La}^{3+}} = 1.14 \text{ \AA}^3$ [51] employed above 1.41 \AA^3 [54] or even 4.82 \AA^3 [53] for the looked for arsenic value 8.47 \AA^3 and 5.07 \AA^3 , respectively. Note that the large magnitude of α_{La} given by Vineis *et al.* [53] has been derived from microwave data involving the full dielectric constants ~ 42 to 48 measured in the frequency range of 4 to 5 GHz. Thus, the corresponding polarizabilities might be strongly affected by low-lying interband transitions which in our approach (see equation (4)) have been already taken into account and the Clausius-Mossotti (Lorenz-Lorentz) relation (equation (9)) has been applied to the background

DC ε_∞ , only, which directly determines the plasma edge $\Omega_p/\sqrt{\varepsilon_\infty} \approx 0.4V$. In contrast the much smaller numbers for $\alpha_{\text{La}^{3+}}$ given in references [51, 54] stand for ionic polarizabilities certainly not affected by such interband transitions.

- [50] Dalgarno A 1962 *Advances in Phys.* **11** 281
- [51] Clavaguéra C and Dognon JP 2005 *Chem. Phys.* **311** 169
- [52] Zhao X, Wang X, Lina H and Wang Z 2007 *Physica B* **392** 132
- [53] Vineis C, Davies, PK, Negas T and Bell S 1996 *Mat. Res. Bull.* **31** 431
- [54] Fraga S, Karwowski J, and Saxena KMS 1976 *Handbook of Atomic data* (Amsterdam: Elsevier)
- [55] The experimentally observed unexpected negative value of $\alpha_{Fe^{2+}}$, if confirmed, is obviously a finite ω -effect. The elucidation of the corresponding ω -dependence of $\alpha_{Fe^{2+}}$ might be also of interest for the pairing mechanism in iron based pnictides and related compounds in addition to the large value of α_{As} confirmed here. However, in the set recommended in reference [48] $\alpha_{Fe^{2+}}$ is positive.
- [56] Anisimov VI, Korotin DMM, Streltsov SV, Kozhernikov AV, Kuneš J, Shorikov AO, and Korotin MA 2008 *arXiv:0807.05471*
- [57] Shorikov AO, Korotin MA, Streltsov SV, Skornyakov SL, Korotin DM, and Anisimov VI 2008 *arXiv:0804.3283v2*
- [58] Laad MS, Craco L, Leoni S, and Rosner H 2009 *Phys. Rev. B* **79** 024515
- [59] We note that an absolutely unreasonable large value of $\varepsilon_\infty = 14.82$ would be obtained, if one would use equation (4) in reference [48]. In the present compound for the anionic polarizability of O^{2-} only $v_c/10$ is available for one O^{2-} -ion. This would cause more than a doubling of the oxygen polarizability: $\tilde{\alpha}_{O^{2-}} = 4.18\text{\AA}^3$ giving rise to the mentioned unrealistic value of ε_∞ exceeding a realistic one by a factor of four.
- [60] Málek J, Drechsler S-L, Nitzsche U, Rosner H, and Eschrig H 2008 *Phys. Rev. B* **78** 060508(R)
- [61] Yatsenko AV, 2001 *Physica B* **305** 287
- [62] Dolgov OV and Maksimov EG 1981 *Uspekhi fizicheskikh nauk* **135** 441
- [63] Coldea A, Fletcher JD, Carrington A, Analytis JG, Bangura AF, Chu JH, Erickson AS, Fisher IR, Hussey NE, and McDonald RD 2008 *Phys. Rev. Lett.* **101** 216402
- [64] Ding H *et al.* 2008 *Europhys. Lett.* **83** 47001
- [65] Zabolotnyy VB, Inosov DS, Evtushinsky DV, Koitzsch A, Kordyuk AA, Sun GL, Park T, Haug D, Hinkov V, Boris AV, Lin CT, Knupfer M, Yaresko AN, Büchner B, Varykhalov A, Follath R, and Borisenko SV 2009 *Nature* **457** 569
- [66] Mamedov TA and de Llano M 2007 *Phys. Rev. B* **75** 104506
- [67] Pou P, Flores F, Ortega J, Pérez R, and Yeyati AL 2002 *J. Phys. Condens. Matter* **14** L421
- [68] Kroll T, Bonhommeau S, Kachel T, Dürr HA, Werner J, Behr G, Koitzsch A, Hübel R, Leger S, Schönfelder R, Ariffin AK, Manzke R, de Groot FMF, Fink J, Eschrig H, Büchner B, and Knupfer M 2008 *Phys. Rev. B* **78** 220502(R)
- [69] Koitzsch A 2009 *private communication*
- [70] Korshunov MM and Eremin I 2008 *Phys. Rev. B* 140509(R)
- [71] Klauss H-H, Luetkens H, Klingeler R, Hess C, Litterst FJ, Kraken M, Korshunov MM, Eremin, Drechsler S-L, Khasanov R, Amato A, Hamann-Borrero J, Leps, Kondrat A, Behr G, Werner J, Büchner B 2008 *Phys. Rev. Lett.* **101** 077005
- [72] Hybertsen MS, Stechel EB, Schlüter M, and Jennison DR 1990 *Phys. Rev. B* **41** 11068
- [73] Eskes H and Jefferson 1993 *Phys. Rev. B* **48** 9788
- [74] Drechsler S-L, Volkova O, Vasiliev AN, Tristan N, Richter J, Schmitt M, Rosner H, Málek J, Klingeler R, Zvyagin AA, and Büchner B 2007 *Phys. Rev. Lett.* **98** 077202
- [75] Nakamura N, Hayashi N, Nakai N, and Machida M 2009 *arXiv:0806.4804*
- [76] Aczel AA, Baggio-Saitovitch E, Budko SL, Canfield PC, Carlo JP, Chen GF, Dai P, Goko T, Hu WZ, Luo JL, Ni N, Sanchez-Candela DR, Tafti FF, Wang NL, Williams TJ, Yu W, and Uemura YJ 2008 *arXiv:0807.1044*
- [77] Park JT, Inosov DS, Niedermayer CH, Sun GL, Haug D, Christensen NB, Dinnebier R, Boris AV,

- Drew AJ, Schulz L, Shapoval T, Wolff U, Neu V, Yang X, Lin CT, Keimer B, and Hinkov V 2008 *arXiv:0811.2224*
- [78] Wälte A, Fuchs G, Müller K-H, Handstein A, Nenkov K, Narozhnyi VN, Drechsler S-L, S. Shulga S, Schultz L, and Rosner H 2004 *Phys. Rev. B* **70**, 174503
- [79] Gurvitch M and Fiory AT 1987 in *Proceedings of the International Conference on Novel Mechanisms of Superconductivity, Berkley*, edited by Wolf SE and Kresin VZ (New York: Plenum) 663
- [80] Hirsch JE and Marsiglio F 1992 *Phys. Rev. B* **45** 4807
- [81] Rüfenacht A, Locquet, J-P, Fompeyrine J, Caimi D, and Martinoli P 2006 *Phys. Rev. Lett.* **96** 227002
- [82] Auer J and Ullmaier H 1973 *Phys. Rev. B* **7** 136
- [83] Anlage SM, Wu DH, Mao J, Mao SN, Xi XX, Venkatesan T, Peng JL, and Green RL 1994 *Phys. Rev. B* **50** 523
- [84] Berthel KH 1973 *Contributions to the Superconductivity, Electronic Structure and Electrical Resistivity of superclean Niobium*, (Dresden: Thesis (in German) University of Technology Dresden, Germany)
- [85] Karakozov A, Maksimov EG, and Pronin AV 2004 *Sol. State Commun.* **129** 425
- [86] Romaniello P, Boeij PL, Carbone F, and van der Marel D 2006 *Phys. Rev. B* **73** 075115
- [87] Zheng XH and Walmsley DG 2008 *Phys. Rev. B* **77** 105510
- [88] Pronin AV, Dressel M, Pimenov A, Loidl A, Roshchin IV, and Greene LH 1998 *Phys. Rev. B* **57** 14 416
- [89] Drew AJ, Pratt FL, Lancaster T, Blundell SJ, Baker PJ, Liu RH, Wu G, Chen XH, Watanabe I, Malik VK, Dubroka A, Kim KW, Rössle M, and Bernhard C 2008 *Phys. Rev. Lett.* **101** 097010. In this work devoted a μ SR study for a $\text{SmO}_{0.82}\text{F}_{0.18}\text{FeAs}$ sample also the data of reference [5] were re-analyzed resulting in a slightly smaller value $\lambda_L(0) = 242(3)$ nm which reduces our λ_{tot} to about 0.46 for all other parameters fixed.
- [90] Khasanov R, Conder K, Pomjakushina A, Amato A, Baines C, Bukowski Z, Karpinski J, Katrykh S, Klauss H-H, Luetkens H, Shengeleya A, and Zhigadlo ND 2008 *Phys. Rev. B* **78** 220510(R)
- [91] Wray L, Qian D, Hsieh D, Xia Y, Checkelsky JG, Pasupathy, Gomes KK, Parker CV, Fedorov AV, Chen GF, Luo JL, Yazdani A, Ong NP, Wang NL, and Hasan MZ 2008 *arXiv:0812061*
- [92] Fletcher JD, Serafin A, Malone L, Analytis J, Chu J-H, Erickson AS, Fisher IR, and Carrington A 2008 *arXiv:0812.3858*
- [93] Analytis JG, Chu J-H, Erickson AS, Kucharczyk C, Serafino A, Carrington A, Cox C, Kauzlarich SM, Hope H, and Fisher IR 2008 *arXiv:0810.5368*
- [94] Vorontsov AB, Vavilov MG, and Chubukov AV 2009 *arXiv:0901.0719*
- [95] Lu DH, Yi M, Mo S-K, Erickson AS, Analytis J, Chu J-H, Singh DJ, Hussain Z, Geballe TH, Fisher IR, and Shen Z-X 2008 *Nature* **455** 81
- [96] Widder K, Berner D, Zibold A, Geserich P, Knupfer M, Kielwein M, Buchgeister M, and Fink J 1995 *Europhys. Lett.* **30** 55
- [97] Drechsler S-L, Rosner H, Shulga SV, Fuchs G, von Lips H, Freudenberger J, Golden MS, Kupfer M, Müller K-H, Schultz L, Fink J, Kaindl G, Eschrig H, and Koepernik K 1999 *J. Low Temp. Phys.* **117** 1617
- [98] Ohishi K, Kakuta K, Akimitsu J, Koda A, Higemoto W, Kadono R, Sonier JE, Price AN, Miller RI, Kiefl RF, Nohara M, Suzuki H, and Takagi H, 2002 *Phys. Rev. B* **65** 14505(R)
- [99] Bommeli F, Degeorgi L, Wachter P, Cho BK, Canfield PC, Chau R, and Maple B 1997 *Phys. Rev. Lett.* **78** 547
- [100] Sonier JE, Callaghan D, Miller I, Boaknin E, Tailleffer L, Kiefl F, Brewer JH, Poon KF, and Brewer JD 2004 *Phys. Rev. Lett.* **93** 017002
- [101] Yao WW and Schnatterly SE, and Testardi L 1978 *Bull. Amer. Phys. Soc.* **23** 302
- [102] Mitrovic B and Carbotte JP 1986 *Phys. Rev. B* **33** 591
- [103] Kihlstrom KE 1985 *Phys. Rev. B* **32** 2891

- [104] MacDougall GJ, Cava RJ, Kim S-J, Russo PL, Savici AT, Wiebe CR, Winkels A, Uemura YJ, and Luke GM 2006 *Physica B* **374-375** 263
- [105] Zhao G-M 2007 *Phys. Rev. B* **76** 020501(R)
- [106] Nagata Y, Mishiro A, Uchida T, Ohtsuka, and Samata H 1999 *J. Phys. and Chem. of Solids* **60** 1933
- [107] Bozovic I, Kim JH, Harris Jr. JS, Hellmann ES, Hartford EH, and Chan PK 1992 *Phys. Rev. B* **46** 1182
- [108] Chang J, Eremin I, Thalmeier P, and Fulde P 2007 *Phys. Rev. B* **76** 220510
- [109] Sonier JE, Sabok-Sayr SA, Callaghan FD, Kaiser CV, Pacradouni V, Brewer JW, Stubbs SL, Hardy WN, Bonn DA, Liang R, and Atkinson WA 2007 *Phys. Rev. B* **76** 134518
- [110] Dahm T, Hinkov V, Borisenko SV, Kordyuk AA, Zabolotny VB, Fink J, Büchner B, Scalapino DJ, Hanke W, and Keimer B 2009 *nature physics* **1180** DOI:10.1038 (online)
- [111] Alexander M 1992 *Electron loss spectroscopy of n-doped High-Temperature superconductors and Related Systems (Ph-Thesis)* (in German) *KfK-Report* **5065** (Karlsruhe: Kernforschungszentrum)
- [112] Tarascon JM *et al.* 1989 *Phys. Rev. B* **40** 4494
- [113] Cappelutti E, Ciuchi S, and Fratini S 2009 *Phys. Rev. B* **79** 012502
- [114] Park SR, Song DJ, Leem CS, Kim CH, Kim C, Kim BJ, and Eisaki H 2008 *Phys. Rev. Lett.* **101** 117006
- [115] Golubov AA, Brinkman A, Dolgov OV, Kortus J, and Jepsen O 2002 *Phys. Rev. B* **66** 054524
- [116] Nicol EJ and Carbotte JP 2005 *Phys. Rev. B* **71** 054501